FACTORS AFFECTING CREEP IN GOLD ON SILICON BI-LAYER MEMS CANTILEVERED BEAMS.

by

NEIL E. WEST

B.S., University of Arkansas, 1997

A thesis submitted to the Faculty of the

Graduate School of the University of Colorado at

At Boulder in partial fulfillment of the requirements

For the degree of Master of Science

Department of Mechanical Engineering

2003

This thesis entitled:

Factors Affecting Creep in Gold on Polysilicon Bi-layer Cantilevered MEMS Beams

written by Neil E. West

has been approved for the Department of Mechanical Engineering

_____

Kenneth A. Gall

_____

Conrad R. Stoldt

Date_____

The final copy of the thesis has been examined by the signatories, and we find that both the content and the form meet acceptable presentation standards of scholarly work in the above mentioned discipline.

West, Neil E. (MS, Mechanical Engineering)

Factors Affecting Creep in Gold on Polysilicon Bi-layer Cantilevered MEMS Beams.

Thesis directed by Associate Professor Kenneth Allen Gall

Abstract

This research identifies factors that contribute to creep in bi-layer gold on polysilicon MEMS beams. Beams used in this research were manufactured using the Multi-User MEMS Process (MUMPs). Their thicknesses were 2μm or 4μm (0.5μm gold on either 1.5μm or 3.5μm polysilicon), these beams were all 20μm wide and ranged in length from 80μm to 280μm in increments of 40μm.

Numerous thermal cycling tests and isothermal hold experiments were conducted at various temperatures. Initial thermal cycling took place at temperatures ranging from room temperature to 275°C, and time durations ranging from 5 to 400 minutes. Isothermal hold experiments were conducted at temperatures ranging from 30°C to 180°C, all isothermal holds have duration of approximately 200 hours. Data was gathered using a Zygo white light interferometric microscope.

It was found that several different stresses act on the beams during thermal cycling and isothermal holds. The stresses can be considered either extrinsic, caused by thermal mismatch stress, or intrinsic, caused by microstructural changes from within the material. Three different internal stresses can act on the bi-layer beams during the hold experiments, gradual creep

which is driven by nano-scale mechanisms, rapid creep which is driven by mechanisms responsible for surface microstructural evolution, and an energy driven recovery mechanism. These three sources of stresses are divided into two regimes. Regime one is a low temperature regime, below approximately 190°C. The curvature response in this regime are gradual creep and recovery, the recovery in regime one takes place slowly due to the lower temperatures. Regime two, the higher temperature regime, experiences internal creep stress that is driven by mechanisms responsible for surface microstructural evolution. This surface evolution driven creep dominates all other creep and recovery mechanisms. Recovery mechanism in regime two takes place very rapidly due the higher temperatures. These factors are acting on the beams at all times. Initial thermal cycling and parameters such as hold temperature and hold time determine which of factor is dominant.

Acknowledgments

I would like to thank Kevin Spark for his technical assistance in gathering data for the hold experiments in this research. I would also like to thank Mike Hulse and Yanhang Zhang for all their support and especially Yanhang for patiently answering my many endless questions.

Chris Dandeneau, Dudley Finch, and Chris Parks for the microscopy images that are seen in this thesis. Ken Gall for his guidance and encouragement.

Most importantly I would like to thank my wife Karen and my children Joseph and Emily, without their support and understanding this work would not have been possible.

Table of Contents

Figures

1. Background

1.1 Micro Electro Mechanical Systems (MEMS)

"Using the fabrication techniques and materials of microelectronics as a basis, Microelectromechanical Systems (MEMS) processes construct both mechanical and electrical components. Mechanical components in MEMS, like transistors in microelectronics, have dimensions that are measured in microns and numbers measured from a few to millions. MEMS is not about any one single application or device, nor is it defined by a single fabrication process or limited to a few materials. More than anything else MEMS is a fabrication approach that conveys the advantages of miniaturization, multiple components and microelectronics to the design and construction of integrated electromechanical systems." Microelectromechanical Systems, a DOD Dual-Use Technology Industrial Assessment December 1995.

Mechanical MEMS devices are designed to provide or detect movement at a microscopic level. Actuation for this movement is provided by numerous means, ranging from thermal mismatch and electrostatic forces, to inertial forces. Detection of this motion is also varied, ranging from measuring change in capacitance to laser reflection, or in some cases direct observation through microscopy. MEMS devices also vary considerably in shape and usage. This thesis investigates only thermally actuated bi-layer cantilevered beams, specifically gold on polysilicon beams.

1.2 Terminology

The following list of terminology is presented to help the reader understand how these terms are used in this research.

Creep: used in this work to describe the loss of beam curvature NOT associated with a change in temperature. The mechanisms include traditional creep, stress relaxation, and strain accumulation.

Recovery: used in this work to describe an increase in beam curvature NOT associated with a change in temperature.

Extrinsic Stress: There is no actual external force applied to the beams in this research. The only true force present is due to the thermal mismatch bi-layer action of the beams. It is assumed all inelastic deformation occurs in the gold layer, therefore, external stress or extrinsic stress is used in this work to describe stress placed on the gold layer by the silicon layer. This stress is mainly due to thermal mismatch between the layers, but any action that results in a curvature, positive or negative, will induce this extrinsic stress.

Intrinsic Stress: Changes in the microstructure of the gold layer that result in an increase or decrease of length of the gold layer are referred to as intrinsic or internal stress. This could result from creep mechanisms or recovery mechanisms.

1.3 Technical Relevance of Creep

MEMS are on the cutting edge of technology. New uses for MEMS are being developed and investigated in both universities and industry. As their usage becomes more widespread, information is needed on their reliability and life cycle characteristics. Creep (time dependent strain accumulation and stress relaxation) has a very large impact on life cycle characteristics of bi-layer beam type MEMS. The beams experience dimensional changes due to creep, which can result in variations from their designed performance characteristics. Beam to substrate distance will change and depending on the application this would result in a capacitance change, variations in pull in voltage, etc. Cantilevered MEMS beams are designed to provide "out of plane" actuation for applications such as switches, sensors, and self-assembly functions. If these devices are actuated by temperature, from either an outside heat source or resistive heating, and held at an elevated temperature they display creep

over a short time, a matter of hours. Over longer periods of time, weeks to years, the beams will also display creep at room temperature. It is important to understand what factors affect creep and to what degree each of these factors contributes to the creep phenomenon in order to design MEMS that have an acceptable life span. Degradation due to creep is not a problem that can be solved in one step. This research will look at some of the factors that affect creep and determine how great their contribution is.

1.4 State of Current Scientific Research

Understanding of micro scale creep is still being developed. As creep in MEMS becomes a concern for reliability, the phenomenon is being researched more frequently. Also, when creep is noted in experiments it is being reported in the subsequent literature. However, there is very little research dedicated solely to creep in MEMS devices.

Earlier work such as Shen and Suresh (1996), investigated creep in multi-layer materials. Their research is driven by microelectronics applications. However, the substrates used in that study are thick compared to MEMS devices and will be have differently than the smaller MEMS devices. Their specimens are 1mm and 1μm metallic film on a 1mm substrate, compared to thicknesses of 0.5μm metallic film on either 3.5μm or 1.5μm polysilicon, which are typical in MEMS devices. Other papers such as Haque and Saif (2002), and Espinosa et al. (2003) and have developed methods for tensile testing of thin metal films. Stress-strain curves were developed and material properties were investigated, but creep was not specifically investigated. The Haque and Saif (2002) papers noted the presence of creep, but it

only occurred when the test specimen was exposed to an electron beam while SEM and TEM images were being taken. They believe the electron beam added sufficient energy to the specimen to activate a diffusion based stress relaxation process.

Larsen et al. (2003) noticed creep behavior while conducting a fatigue test of LIGA nickel. They conducted two different annealing processes on the test structures. Annealing at 120°C for sixty minutes did not cause any material property changes in the test specimens. Annealing at 230°C for sixty minutes resulted in reduced creep behavior and better fatigue response. He credits both of these changes to grain growth during the annealing process. Cho et al. (2003) measures mechanical properties of LIGA nickel at room temperature and at elevated temperatures. Creep tests were conducted at temperatures ranging from 265°C to 400°C. The results of these creep tests are plotted in Figure 1. The applied stress in these experiments is 110 MPa, which at 265°C this is only half of the nickel's yield strength. Even though the applied stress was only half of the yield strength, considerable creep (0.2%) was observed within one hour.

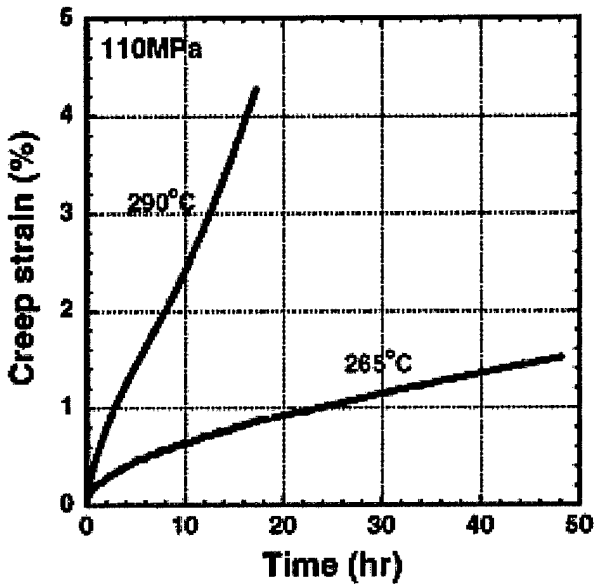

Figure 1. Creep curves at 265 and 290°C under the stress of 110MPa. The accumulation of creep deformation is significant, even at these modest stresses and temperatures. (Cho et al. 2003)

The only paper found that looks specifically at creep in gold on polysilicon bi-layer MEMS beams was Zhang and Dunn 2001. This is one of the very few papers that specifically addresses creep in MEMS bi-layer beam structures. To examine creep experimentally they use gold on polysilicon beams made with the same manufacturing process and very similar geometry, 0.5μm gold film on either 1.5μm or 3.5μm polysilicon, as the beams used in this thesis. Rather than applying an external load to the beams as in the other studies, Zhang and Dunn use stress that results from thermal mismatch between the gold and polysilicon layers of the beams. The structures were heated to 190°C, cooled back to 120°C, and isothermally held for 1000 hours. All structures that were tested in their experiment showed effects of creep during the isothermal hold. In an effort to model the creep, Zhang and Dunn used the Abaqus finite element code. The stress relaxation process was modeled using a power law creep equation.

$$\dot{\varepsilon} = A\sigma^n$$

where

$\dot{\varepsilon}$ =creep rate σ= stress in gold

A and n =creep and material constants of the gold

The model was formed by fitting the experimental data from the 0.5 μm gold on 3.5 μm polysilicon beams to determine the constant "A" and exponent "n" values. Zhang and Dunn show that for specific beam geometry (thickness, length, and width), hold temperature, and initial thermal cycling, a power law model could be fit to measured data. It is important to note that the material constant "A" in the model had to be modified to account for the change in geometry between the 1.5μm polysilicon and the 3.5μm polysilicon beams.

1.5 Analysis and Behavior of Bi-layer Beams

To understand factors affecting creep in bi-layer MEMS beams, it is important to first understand how they deform. The principle of deformation is based on different thermal expansion coefficients of the bi-layer materials. Deformation depends on beam geometry, change in temperature, elastic modulus of the two materials, and the magnitude of the difference in the thermal expansion coefficients. Gold on polysilicon beams are used for this research. Gold has thermal expansion coefficient values ranging from $14.1\text{x}10^{-6}$ 1/°C to $15.1\text{x}10^{-6}$ 1/°C. Silicon has thermal expansion coefficient values ranging from $3.21\text{x}10^{-6}$ 1/°C to $4.68\text{x}10^{-6}$ 1/°C. This

range in values is related to the temperature dependence of the coefficients (Zhang and Dunn 2001).

As the beam is cooled, the gold will try to shrink more than the polysilicon because the gold has a larger thermal expansion coefficient. Because the two layers are bonded and cannot shrink independently a tensile stress is created in the gold and compressive stress in the polysilicon. The beams will curve up in order to relieve this stress. By the same principles the beams can be forced to curve downward by heating them. Several studies have determined ways to relate curvature to stress in the layers and mismatch stress between the layers. Classical papers such as Stoney (1909) and Nix (1988) relate curvature of thin films on thick substrates to stresses within the film. Stoney and Nix's observations have been used in microelectronics but are either unusable or must be used with modification when the thin film's thickness is comparable to the thickness of the substrate.

Timoshenko (1925) relates curvature to stress in bimetallic structures of various materials and geometry,

$$K = \frac{1}{\rho} = \frac{6(\alpha_2 - \alpha_1)(t - t_0)(1+m)^2}{h\left(3(1+m)^2 + (1+mn)\left(m^2 + \frac{1}{mn}\right)\right)}$$

Where:

$\frac{t_1}{t_2} = m$ $\quad$ $\frac{E_1}{E_2} = n$ $\quad$ $n = t_1 + t_2$ $\quad$ $\rho = radius\ of\ curvature$

$t_i = layer\ thickness$ $\quad$ $K = curvature$ $\quad$ $E_i = Modulus\ of\ elasticity$

This relationship has been used effectively in MEMS bi-layer beams to determine some mechanical properties such as Young's modulus and Poisson's ratio (Pamula et al 2001).

A more recent publication (Dunn and Cunningham 2003) provides equations to relate curvature to mismatch strain in bi-layer MEMS plates. They also demonstrate that applying the plate theory gives more accurate curvature results in beams than the traditional beam theory in predicting curvature.

$$k = K\varepsilon_m$$

Where

$$K = \frac{6hm}{t_1}\left[\frac{1+h}{1+2hm(2+3h+2h^2)+h^4m^2}\right]$$

$$t_i = layer\ thickness \quad h = \frac{t_2}{t_1} \qquad M_i = Biaxial\ Modulus \quad M_i = \frac{E_i}{1-\nu_i}$$

$$m = \frac{M_2}{M_1} \qquad k = curvature$$

$$\varepsilon_m = MismatchStrain$$

$$Thermal\ Mismatch\ Strain = \Delta\alpha\Delta T = (\alpha_{Si} - \alpha_{Au})*(T_O - T)$$

This equation is dependent on geometry and material properties of the beam. Since the beam dimensions and materials (gold and silicon) are known, mismatch strain can be calculated from the experimentally determined curvature. The equation assumes zero strain when the beam has zero curvature. That is, if the gold and polysilicon layers were separated both layers would be the same length. It is also important to note that this equation is only valid in the elastic region of deformation.

In other words, the equation is not meant to predict curvature during inelastic deformation. This may seem counterintuitive for experiments dealing with inelastic creep deformation, but the equation can still be meaningful if inelastic strains are lumped into the mismatch strains. The beams experience a curvature decrease as a function of time during the isothermal hold. No input factors, such as hold temperature or thermal processing, change during the hold. This decrease in curvature is attributed to an inelastic deformation process. We can use the equation to track change in inelastic mismatch strain by taking the difference in curvature between two points in time. This change of curvature over a given time period is due to inelastic deformation that takes place during the same time period.

In order to verify the equation was valid for the beams used in this research, curvature was calculated and compared to experimentally measured curvature. The first step in this process was to calculate mismatch strain using the difference in thermal expansion coefficients and the difference in temperature between a reference temperature

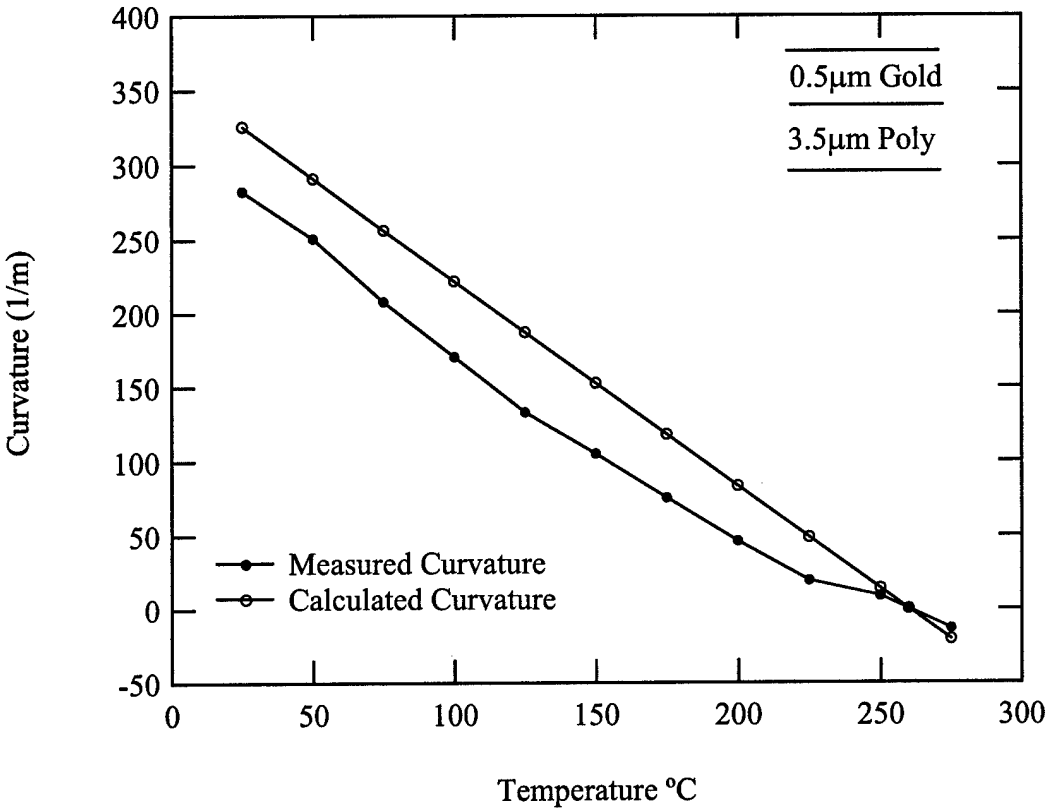

Figure 2. Mismatch Strain Equation Accuracy for 3.5μm poly beams

and the temperature of a known curvature measurement. Using experimental data, the temperature that had a corresponding zero curvature was calculated and set as the reference temperature T_o. By subtracting the temperature at each known experimental curvature value, a mismatch strain was determined in both the 1.5μm polysilicon beams and the 3.5μm polysilicon beams. Curvature was then calculated using this mismatch strain. These calculated curvatures were compared to the measured curvatures at each temperature. The measured curvature is plotted, Figures 2 and 3, on the same graph as

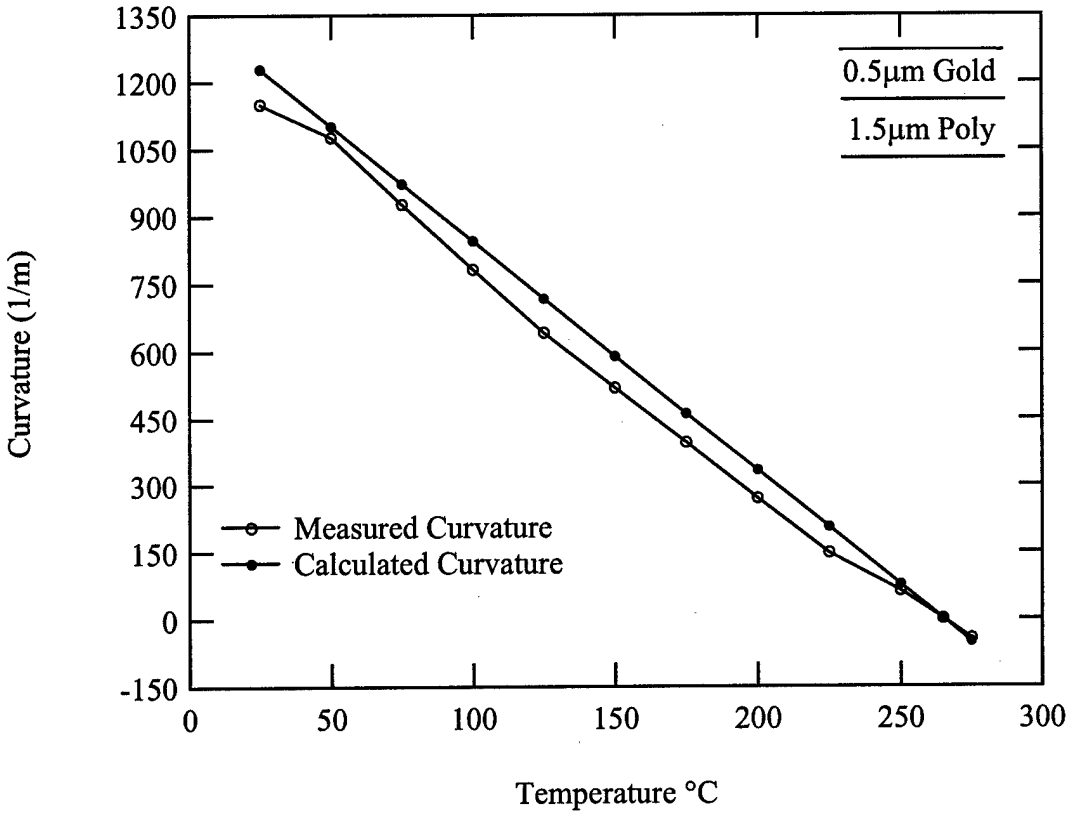

Figure 3. Mismatch Strain Equation Accuracy for 1.5μm poly beams

calculated curvature in order to determine the accuracy between experimental values and the calculated values. Each individual data point should be thought of as an instantaneous curvature, because the equation is not used in this step to determine change in curvature. The calculated values merely predict curvature based on the given reference temperature and the temperature at which each measurement was taken. These plots show the equation successfully predicts the average curvature throughout the temperature range of the experimental data for both the 1.5μm poly and the 3.5μm poly beams.

1.6 Scope of Study

The scope of this study is to investigate factors that contribute to creep in bi-layer MEMS beams. By varying curvature states in the beams and thermal environment, this research will try to identify some of the factors and determine the magnitude to which they affect creep.

1.7 Testing

A thermal chamber is used to heat the MEMS beams to a specified temperature and then cool them back to a specified isothermal hold temperature. They are then held for approximately 200 hours. Curvature measurements are taken during initial heating and cooling cycle as well as during the hold period to determine how much the curvature changes. The data obtained from these experiments is then plotted and analyzed. Test procedures are covered in greater detail in section 2.3

2. Methodology

2.1 Specimen and Specimen Preparation

2.1.1 Manufacture process

Beams used in this research were manufactured using the MUMPs process (Multi-User MEMS Process) Koester et al 2001. In this process layers of material are deposited on a surface, then these layers are selectively etched and new layers applied in order to create structures. The MUMPs process can utilize up to three poly-silicon layers "Poly 0", "Poly 1", and "Poly 2". Between each layer deposition, a masking and etching process takes place. This allows the manufacturing of structures by removing selected portions of each poly-silicon layer.

The MUMPs process starts with an n-type (100) silicon wafer, a nitride layer is deposited using a low-pressure chemical vapor deposition system. After the nitride is deposited the poly-silicon layers are sequentially deposited. The beams used in this research did not require the "Poly 0" layer. Only "Poly 1" and "Poly 2" layers were needed. Between each poly-silicon layer, a deposition of masking material, patterning of the mask, and an etching process takes place to remove the desired areas of the poly silicon. Also between each poly-silicon deposition, a phosphosilicate glass (oxide layer) is deposited and an annealing process takes place. These chips are annealed two times at 1050°C for an hour each time. After the final poly-silicon layer is etched a final "lift off" masking takes place. A thin layer of chromium, approximately 500 angstroms, is deposited as a bonding medium and

then a 0.5μm layer of gold is deposited at approximately 100°C. Due to the layers of different materials that are built up and the high temperatures the chip experiences during manufacturing, the beams have residual stresses manufactured into the structure. The annealing process reduces some of the stresses in the various layers. However, final residual stresses can vary from 140 MPa tensile to 30 MPa compressive stresses through out the MEMS structure.

2.1.2 Release Process

Before the beams can move freely the chip must be released. The release process removes the oxide layers. This is accomplished through a multiple step chemical process. The first steps use acetone to remove a protective photo resist from the chips, then alcohol and water are used to remove the acetone. After the photo resist is removed hydrofluoric acid (HF) is used to etch away the oxide layer. This is the step that physically removes the oxide layer and allows the beams to move. Great care must be taken when using HF, it will destroy glass containers and can be fatal if it contacts the skin. The chip is immersed in the HF for approximately two minutes, then placed in a methanol and water solution, then to pure methanol to remove the HF.

The final step in the release process is to dry the chip. If the chips were allowed to air dry the liquid underneath the beams would pull the beams down to the substrate as the liquid evaporated. If this were to occur the beams would remain stuck to the substrate even after all the liquid had evaporated. This phenomenon, beam sticking to the substrate, is stiction. In order to avoid stiction the chips are

placed directly into a critical point CO_2 dryer. The dryer chamber is initially filled with methanol and cooled to 4°C. After the chamber is cooled all methanol is flushed out and replaced with liquid CO_2. The dryer chamber is pressurized and slowly heated to the CO_2 critical point (Approx. 31°C and 74 bar), the CO_2 flashes from the liquid phase to the gas phase. This prevents any liquid surface tension effects from pulling the beams to the substrate. The CO_2 gas is then drained from the dryer chamber and the release process is completed.

2.2 Equipment

Only two major pieces of equipment are used in this research. Thermal chambers that are used to heat and cool the chips, and a Zygo brand interferometric microscope to record surface profile data of the chip. The Zygo interferometric microscope uses a beam of white light. This light beam is split into two separate beams, one is reflected off the surface of the chip and the other is reflected off a reference surface. These two beams are then reflected back to a camera which converts the white light images into a digital signal. This signal is processed using MetroPro software which utilizes the difference between the two light beams to create a three dimensional image of the surface. MetroPro software gives many options for measuring surface features and processing the data that is acquired during the measurements (Fig 4). The three dimensional surface image is recorded digitally for each of the surface profile measurements taken. These images are saved and the beam curvature measurements can be made during the experiment or after each experiment is complete. One of the data processing options allows easy curvature

measurements of the beam surface. A "Slice Information" line is placed on a portion of the beam image in the "Surface Map" window and the "RadCrv" option gives the radius of curvature. The units chosen for the radius of curvature are millimeters and a numerical result is given in the "Surface Profile" window. It is customary to use curvature K rather than the radius of curvature. This is easily obtained in a spreadsheet by inverting the radius of curvature and multiplying by 1000 to give curvature in inverse meters.

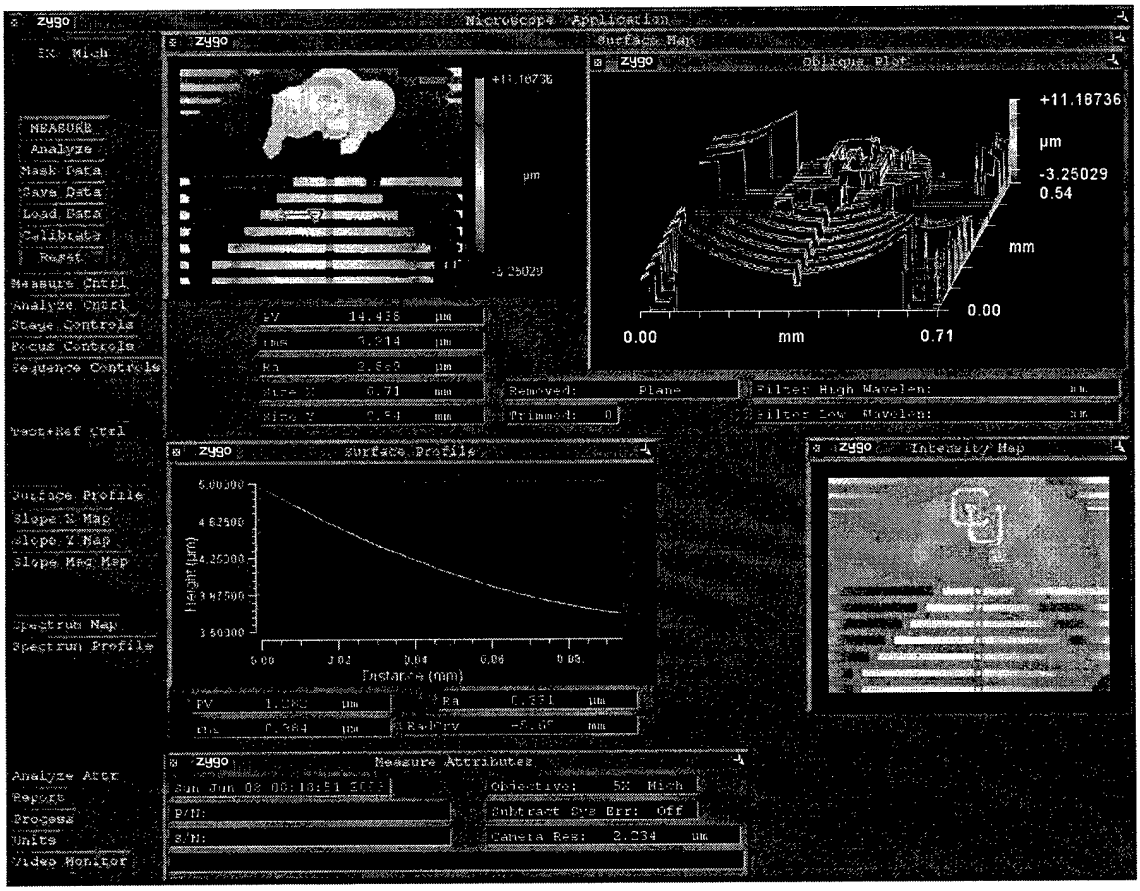

Figure 4. Example of information screen with images from Zygo microscope using Metro Pro software.

Utilizing two thermal chambers allows two experiments to be conducted simultaneously. These thermal chambers have a resistive heating surface inside the chamber that is connected to a controller which maintains the desired temperature. The thermal chambers are small enough to be placed on the microscope stage and surface profile measurements can be made through a glass window in the top of the thermal chamber. The first chamber is custom built and has no forced cooling system, which makes it ideal for hold experiments but very cumbersome for cycling experiments. It's temperature resolution is 1°C and has a range from room temperature to well above 500°C. The second chamber is a commercially available Instec STC 200. This chamber has a forced cooling system which consists of fluid passages within the chamber that fluid can be pumped through. This chamber is well suited for hold experiments as well thermal cycling. It has a resolution of 0.1°C with a range from –196°C (if liquid nitrogen is used as the coolant) to well above 500°C. This research uses temperatures ranging from room temperature to 225°C, so both chambers are well suited for this research.

2.3 Creep Tests

Initial thermal cycling and hold experiments were conducted using an interferometric microscope (Zygo) and two thermal chambers. All the thermal tests were conducted in a similar manner but used different maximum temperatures and different hold temperatures. As discussed in section 1.4 a change in temperature of the beams will result in a change of curvature. In an attempt to isolate the effect of either stress due to curvature or the effect of hold temperature, several experiments

were planed with various hold temperatures and various maximum temperatures. Experiments sets were either all held at the same temperature after being exposed to various maximum temperatures or heated to the same maximum temperature and held at various temperatures. A few experiments were conducted to further investigate interesting observations noted during other experiments. After the maximum and hold temperatures were determined for each experiment, a chip is removed from its storage container and placed on the heating surface in one of the thermal chambers. The glass covered opening in the chamber allows all the measurements to be made without removing the chip from the isothermal hold and causing undesired thermal cycling. Initial thermal cycling is started at room temperature, and heated in increments of about 50°C. At these 50°C intervals the heating process is paused long enough (Approximately 5 minutes) to make surface profiled measurements of the chip using the Zygo microscope. The time and temperature are recorded in a log, and a file containing the surface profile information is saved with the time/date information as the file name. When the maximum temperature is reached another measurement is taken and again at regular intervals during the cooling process until the chip is cooled to the isothermal hold temperature. The chip is then held for approximately 200 hours or about eight and a half days. Initially, a large decrease in curvature is observed and the rate of change slowly decreases through out the remainder of the hold period. Due to this initial high rate of creep several measurements are taken on the first day of the experiment. After approximately the first 48 hours only two measurements are taken each day up

to approximately 120 hours. At least one measurement is then taken each day for the remainder of the hold time.

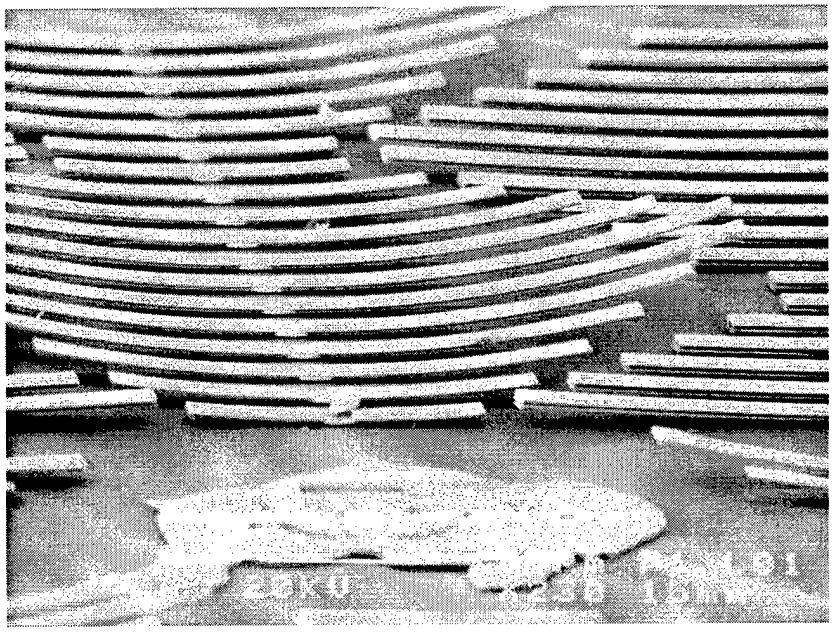

Figure 5. Image of MEMS Structures.

Each MEMS chip has 216 beams manufactured on it. 108 of these beams are 0.5μm gold on 1.5μm poly silicon, and 108 beams are 0.5μm gold on 3.5μm poly silicon. Usually some of the MEMS beams will be damaged or stuck to the substrate, and sometimes debris such as dust particles will be on the surface. For data collection, a section of approximately 24 beams are chosen that has either no damage or the least amount of damage and surface discrepancies. All images through out the 200-hour isothermal hold are taken of this same section. In order to minimize the effect of experimental uncertainties each data point is an average of six or eight

curvatures. Two interferometric images are taken of the same section of beams, and three or four beams are chosen and observed for the duration of the experiment. Two measurements of these beams are used to calculate the average curvature that is used for the individual data point. The beams are all 20μm wide and vary in length from 80μm to 280μm in increments of 40μm. (Fig 5). Curvature of the MEMS beams has been found to be

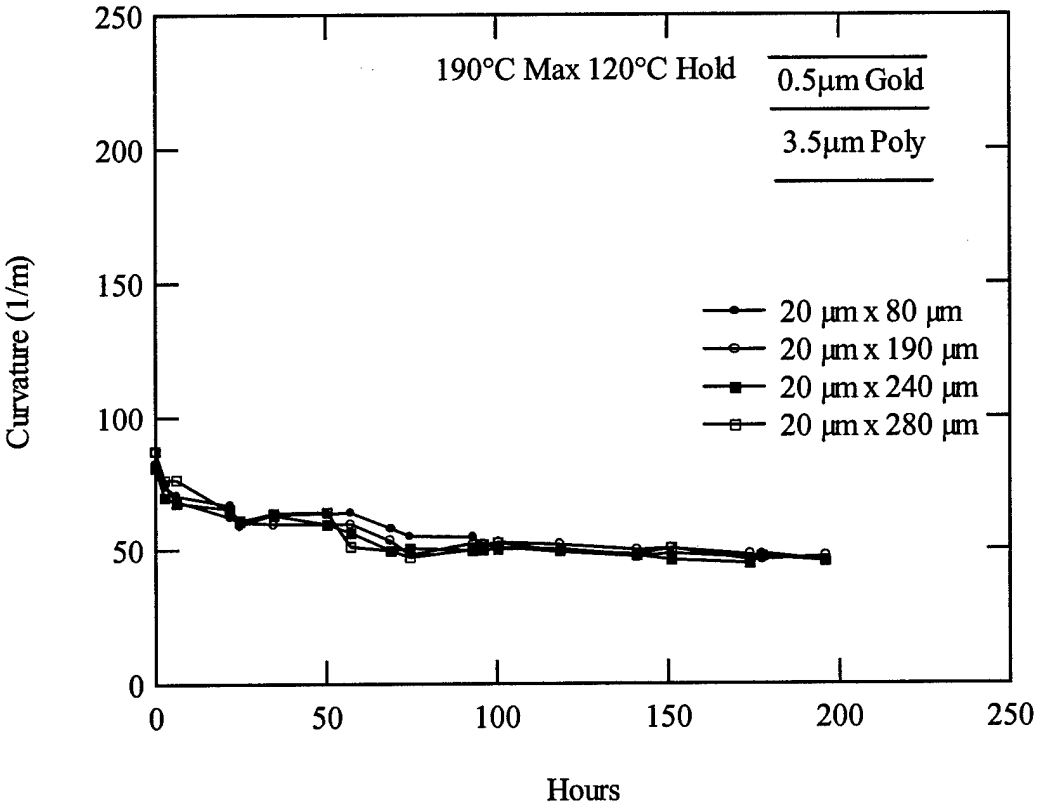

Figure 6. Effect of Beam Length on Creep.

independent of beam length. The change in curvature over time is very consistent between the different length beams (Fig 6). This allows the average of the six or

eight curvature measurements to be an accurate representation of the curvature and the change in curvature for the duration of the hold experiments.

In order to ensure data accuracy, a series of data analysis experiments were run. Variability sources were broken down into categories and each was examined for its contribution to the overall uncertainty in the data. The first area considered was the accuracy of the Zygo interferometric microscope. A series of ten readings were taken of the same spot on the same beam from ten individual images. These readings were taken over approximately one minute's time in order to remove the effects of creep. If 100% accurate, these readings should have been identical, however as to be expected, there were small variances found in the readings of approximately 3.4%.

Next we examined the length of the "slice information" line used to find the radius of curvature of the beams. This line provides the data points averaged by the MetroPro software when calculating the radius of curvature. Intuativly, by making the line longer, more data points would be averaged, thus mapping beam behavior more accurately. To check the accuracy of our data, the 190°C max temperature, 120°C hold temperature data was re-taken from the same beams as measured previously but with a blank long "slice information" line instead of a blank long line. We found the data taken with a longer "slice information" line to be nearly identical to the data taken with a shorter "slice information" line thus reaffirming our original data's accuracy.

3. Results

3.1 Thermal Cycling Response

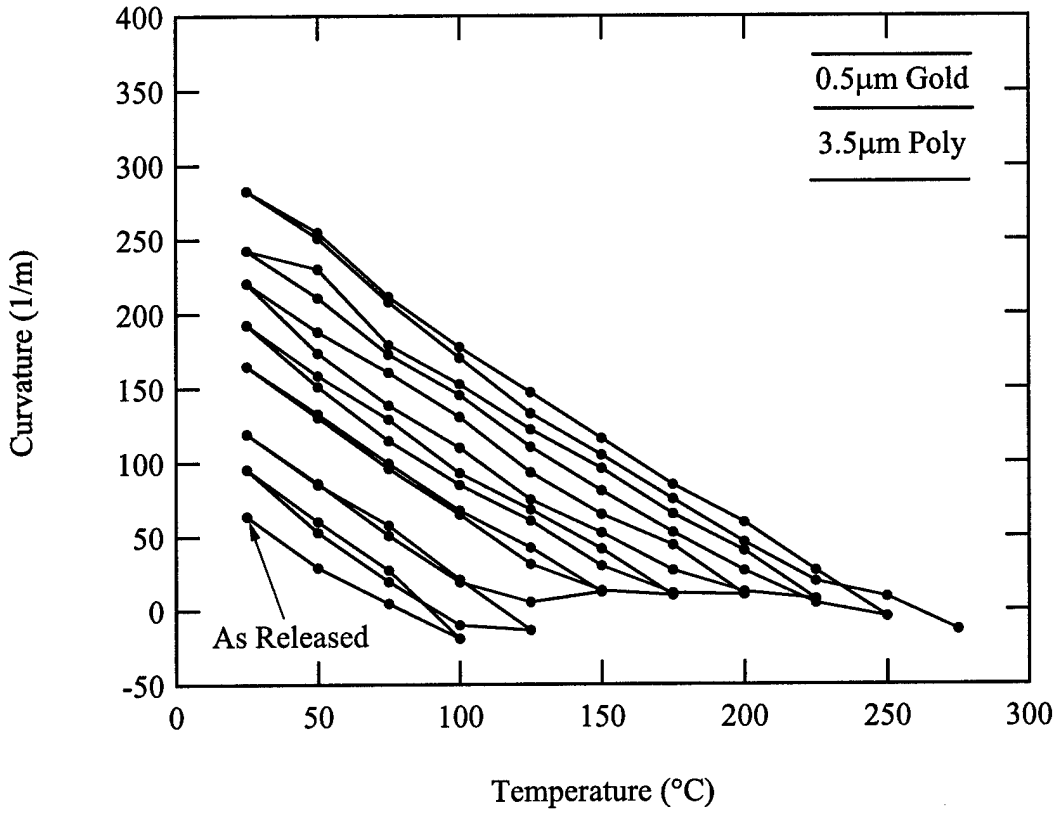

Figure 7. Initial Thermal Cycling Response of 3.5μm Poly Beams. (Gall et al. 2003)

Figure 7 shows the curvature versus temperature behavior of the 3.5μm polysilicon beams. The "as-released" chip is heated from room temperature to 100°C then cooled back to room temperature. This is repeated for progressively higher temperatures. As evident from figure 7 the curvature temperature relationship can become nonlinear during the initial heating process. However, when the beams are cooled back to room temperature they follow a linear curvature temperature

relationship. They also follow the same linear response when they are reheated to the previously high temperature. When heated past the previously high temperature the beams again experience a nonlinear curvature temperature relationship to the subsequent higher temperature. MEMS beams obey the same nonlinear relationship regardless if the beams are heated directly to the high temperature or if they are heated and cooled incrementally to the higher temperature.

The nonlinear curvature relationship changes through the course of the initial heating process. The beams experience three different curvature temperature relationships while being heated from room temperature to the maximum temperature of 275°C. The beam curvature decreases rapidly while they are being heated to approximately 100°C. After reaching 100°C the beams will begin recovering curvature until they are heated to approximately 175°C. At this point the beams again lose curvature as they're being heated, but at much slower rate than the initial heating. This loss in curvature continues through the remainder of the experiment. Figure 8 shows the curvature versus temperature behavior of the 1.5μm polysilicon beams.

Curvature response of both the 1.5μm and 3.5μm polysilicon beams is qualitatively similar, the thinner beams, as one would expect, have much greater curvature than the thicker beams. Response of the two beams is essentially the same except for the magnitude of the curvature. By using the plotted results of this experiment, a desired curvature at a particular hold temperature can be obtained by heating the beams to the appropriate maximum temperature. Or if a particular

maximum temperature and curvature combination is desired for an experiment, the hold temperature can be manipulated to produce the appropriate curvature.

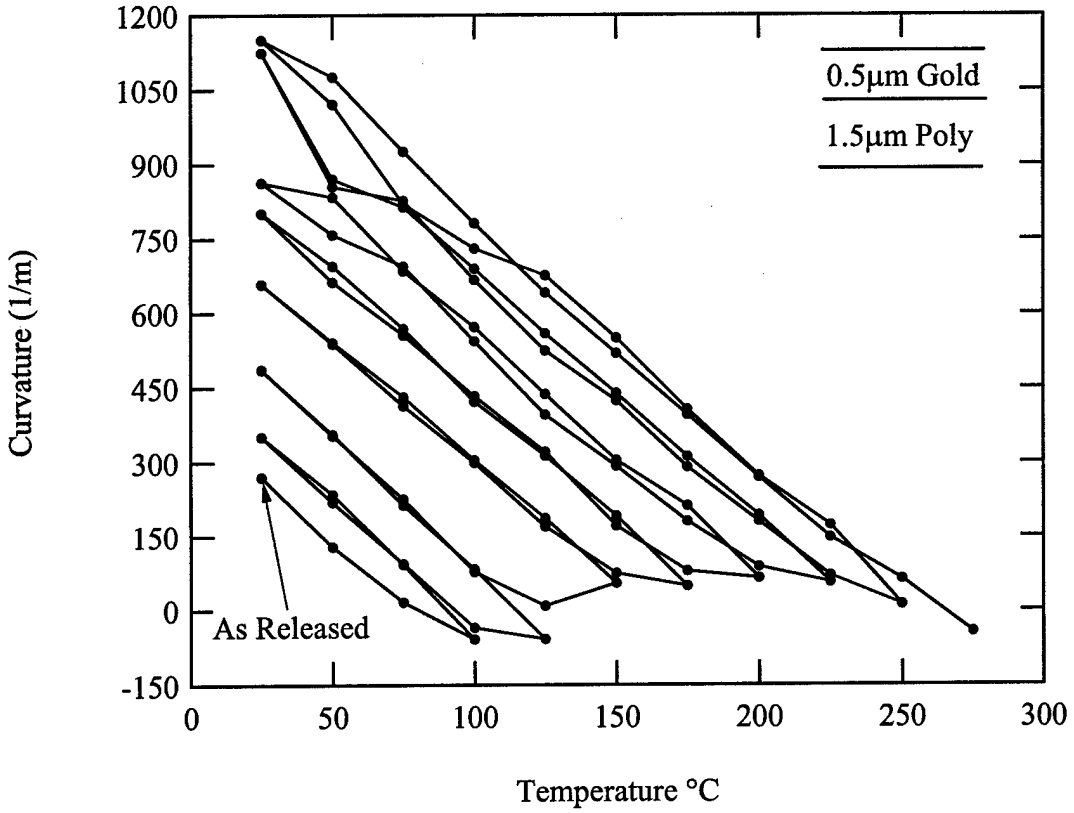

Figure 8. Initial Thermal Cycling Response of 1.5μm Poly Beams (Gall 2003)

3.2 Initial Curvature

Figures 9 and 10 show curvature resulting from the initial thermal cycle process of the isothermal hold experiments. The beams in these plots follow the behavior described in the previous section. In the 190°C maximum temperature experiments, the initial thermal cycle process heats the beams past the point of initial rapid curvature loss just to the point that beams stop recovering curvature, before being cooled back to the respective isothermal hold temperatures.

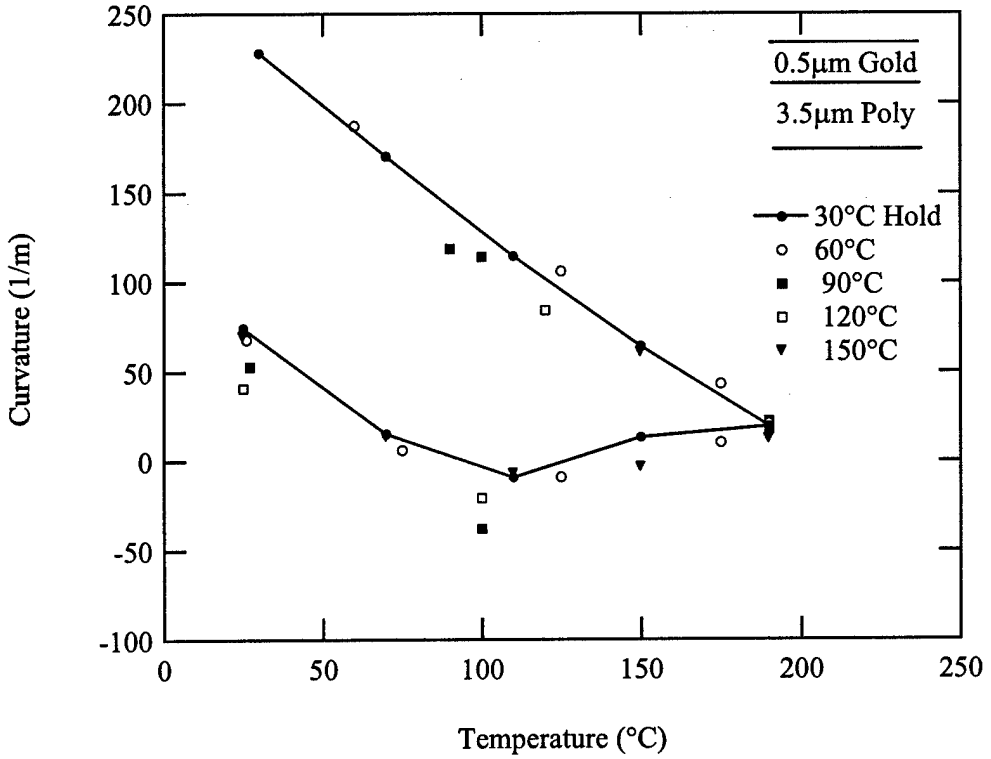

Figure 9. Initial Curvature of 190°C Max Temperature Hold Experiments

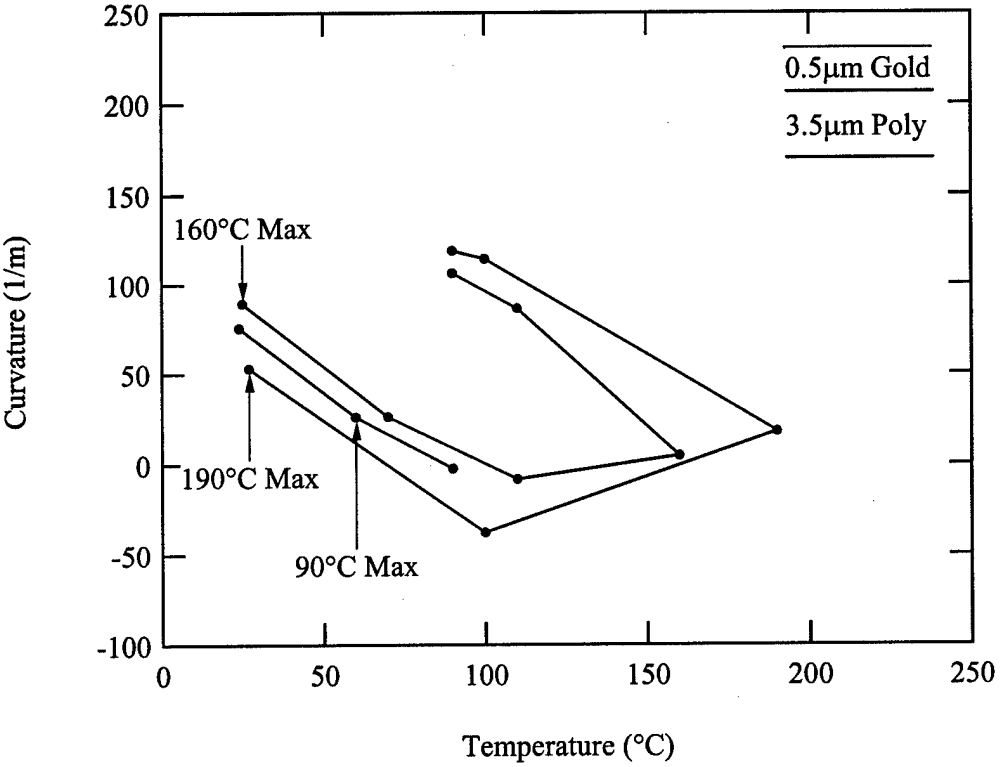

Figure 10. Initial Curvature of 90°C Hold Temperature Experiments

In the 90°C maximum hold experiments, the beams that are heated only to 90°C are not allowed to reach the point that the beams stop rapid loss of curvature upon the initial heating. In both initial curvature plots there is a slight spread in curvature values at the same temperatures. The variance is partially due to the different stresses from the different MUMPs runs. Even though there is some variability between the data points all of the beams, regardless of manufacturing stresses, follow the same trends established in the ladders plots.

3.3 Different Hold Temps, Same Max Temp

In the first group of experiments, all the beams were heated to 190°C and cooled backed to various hold temperatures. The results of this experiment set are plotted in Figure 11. This plot shows curvature verses hold time for several different isothermal hold temperatures. Because the beams are all heated to the same maximum temperature, the initial curvature is successively larger for each lower hold temperature. Following the beam behavior illustrated in figures 7 and 8, the beams all have the same curvature when they are at 190°C. As each beam is cooled to their respective hold temperatures the beams that are cooled more will have a larger curvature. Two important observations from this experiment are different curvature behavior of the beams during the first few hours of the hold compared to the behavior during the remainder of the hold and the behavior of the beams held at 150°C. In the initial stages of creep, up to approximately 20 hours, the curvature changes rapidly, usually decreasing but sometimes a combination of increasing and decreasing occurs, and after approximately 20 hours all of the curvature change

approaches a steady state. The four lower temperature holds 30°C, 60°C, 90°C, and 120°C continue to creep through out the hold period. After they reach a steady creep rate they maintain this rate and display no other behavior worth note. The second important observation concerns the beams that were held at 150°C. They display two stages of curvature behavior, but the initial stage

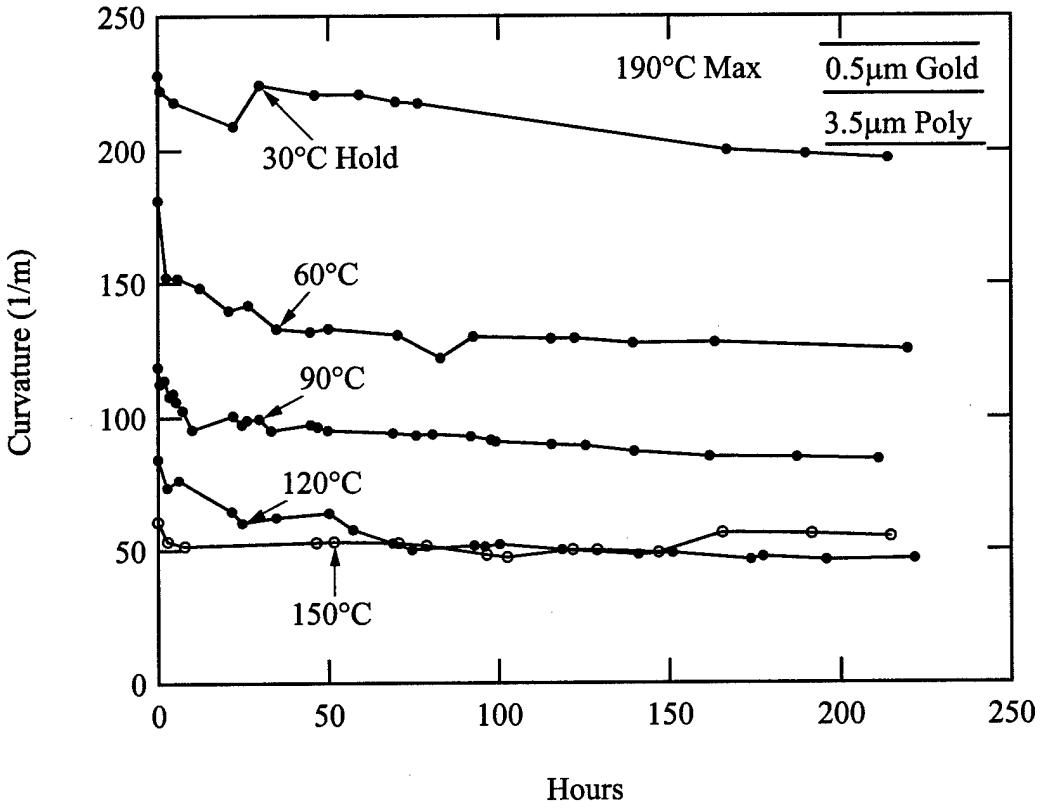

Figure 11. Results of Creep Experiments With 190°C Max Temperature and Various Hold Temperatures.

is very short and very little curvature decrease is noted. In the second stage these beams do not show a decrease in curvature and increase slightly starting at approximately 150 hours. From approximately 75 hours to 150 hours the 120°C beams and the 150°C beams have approximately the same curvature, but the 120°C

beams continue to creep and the 150°C beams begin to recover. The beams held at a higher temperature reach the end of the experiment with a higher curvature.

3.4 Different Max Temps, Same Hold Temps

In this set of experiments the beams experience the same isothermal hold temperature after being heated to different maximum temperatures. Results of the 120°C degree hold experiment set are shown in Figure 12. In this experiment set all the beams are held at the same temperature. Therefore, initial curvatures are successively greater for successively higher maximum temperatures. After the initial erratic curvature behavior stage both the 220°C maximum and the 190°C maximum beams experience similar rates of change in curvature. A very interesting observation from this experiment set is that the 3.5μm polysilicon beams that were heated to 160°C maximum do not creep after the primary creep stage. In order to show that this was not an anomaly the experiment was repeated and the same results were noted. For hold time from approximately 20 hours to 60 hours the 160°C maximum beams had similar curvature as the 190°C maximum beams, but the 190°C maximum beams continue to lose curvature at the same rate as the 220°C maximum beams after the 60-hour point.

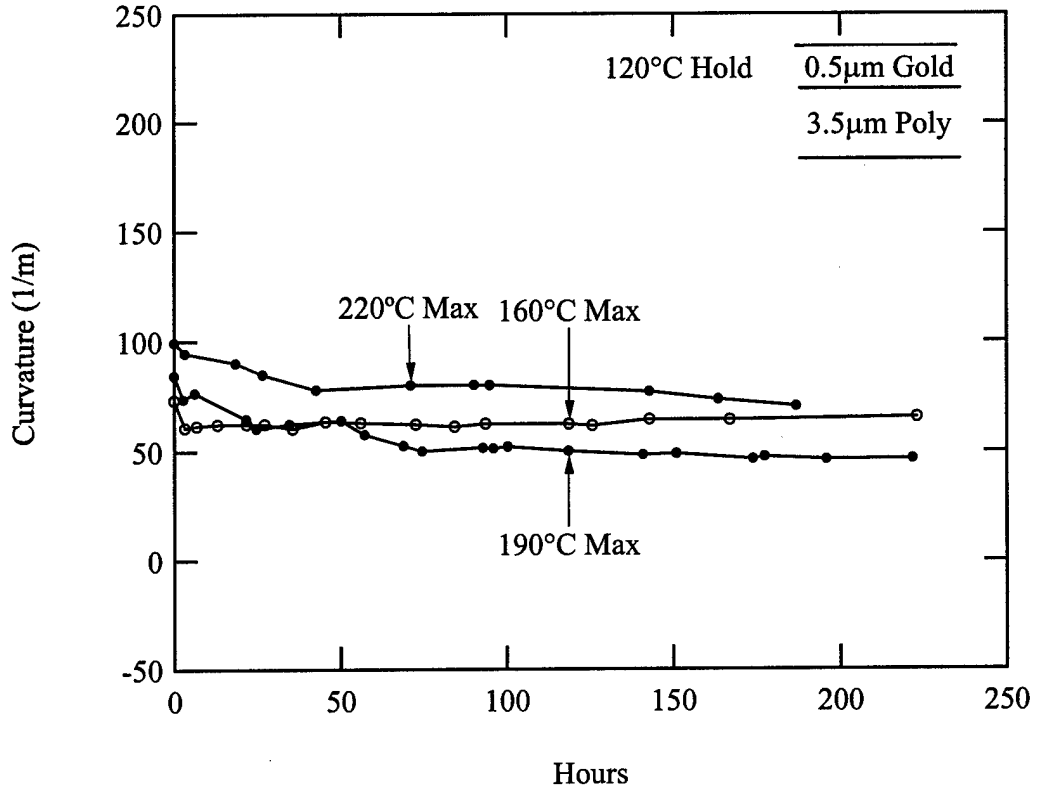

Figure 12. Results of Creep Experiments with 120°C Hold and Various Max Temperatures.

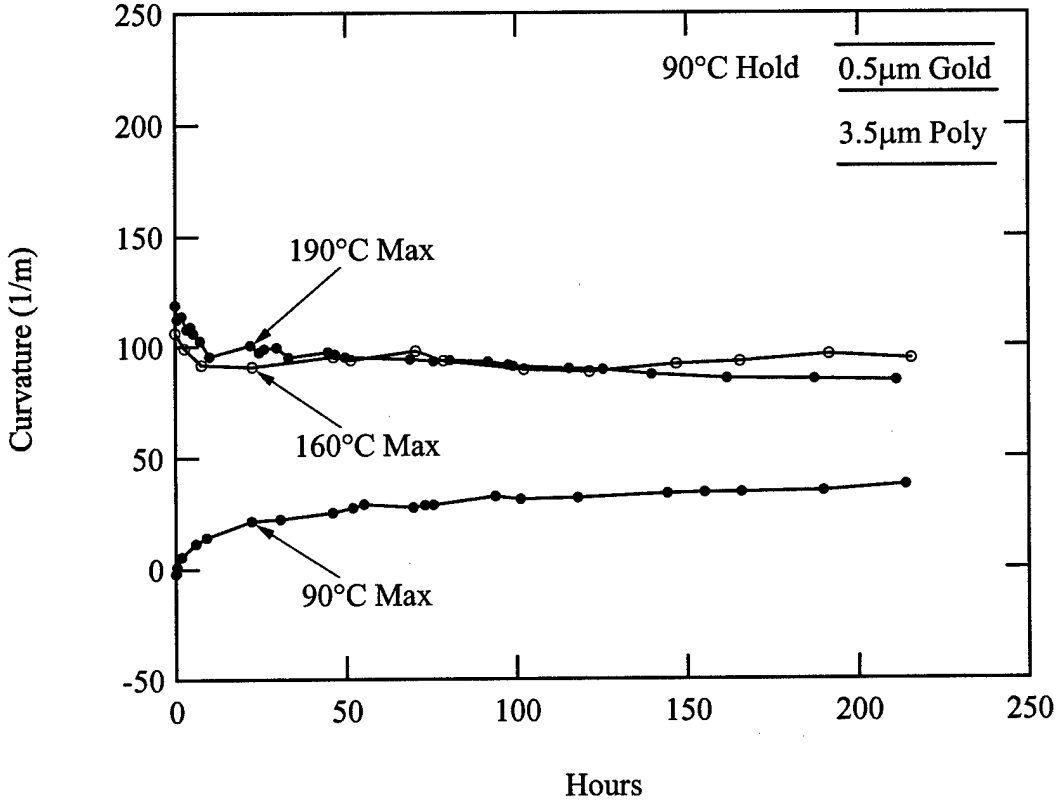

Figure 13. Results of Creep Experiments with 90°C Hold and Various Max Temperatures.

The third experiment set basically takes the second experiment to an extreme case. Beams are held at 90°C after being exposed to different maximum temperatures The results of this experiment are plotted in Figure 13. Again, because the beams and are held at the same temperature they show successively higher initial curvatures for successively higher maximum temperatures. The most obvious observation from this experiment is that the 3.5μm polysilicon beams that were heated to 90°C maximum recover curvature, going to a higher curvature through the duration of the experiment. The beams that were heated to 160°C perform as expected based on the 120°C hold experiments. The 160°C maximum beams initially start out at a lower curvature than the 190°C maximum beams but after initial creep, the 160°C maximum beams stop losing curvature through the remainder of the experiment. Similar to the phenomena seen in the 120°C hold, both the 190°C maximum and the 160°C maximum beams have approximately the same curvature for part of the experiment but the 190°C maximum beams continues to lose curvature after the 160°C maximum beam stopped losing curvature.

3.5 190°C Maximum 150°C Hold, With 400 Minute 190°C Hold

The 150°C Hold in the first group of experiments did not show the effects of creep during the isothermal hold. In order to further investigate this phenomenon an additional experiment was devised that added a 400 minute 190°C isothermal during the initial thermal cycling. The initial thermal cycling process was stopped at 190°C for 400 minutes before the beams were cooled to their final holding temperature of 150°C. The results of this experiment are shown in figures 14 and 15.

During the initial thermal cycle the beams were held at 190°C for 400 minutes instead of cooling them directly back to their hold temperature. During the 400 minute hold the beams recover approximately 50 1/m of curvature. Other than the recovery of curvature the beams behave in the same manner as all other beams during the initial thermal cycle. Taking into account data collection uncertainties, the beams follow the same nonlinear temperature curvature relationship to the maximum temp. They then

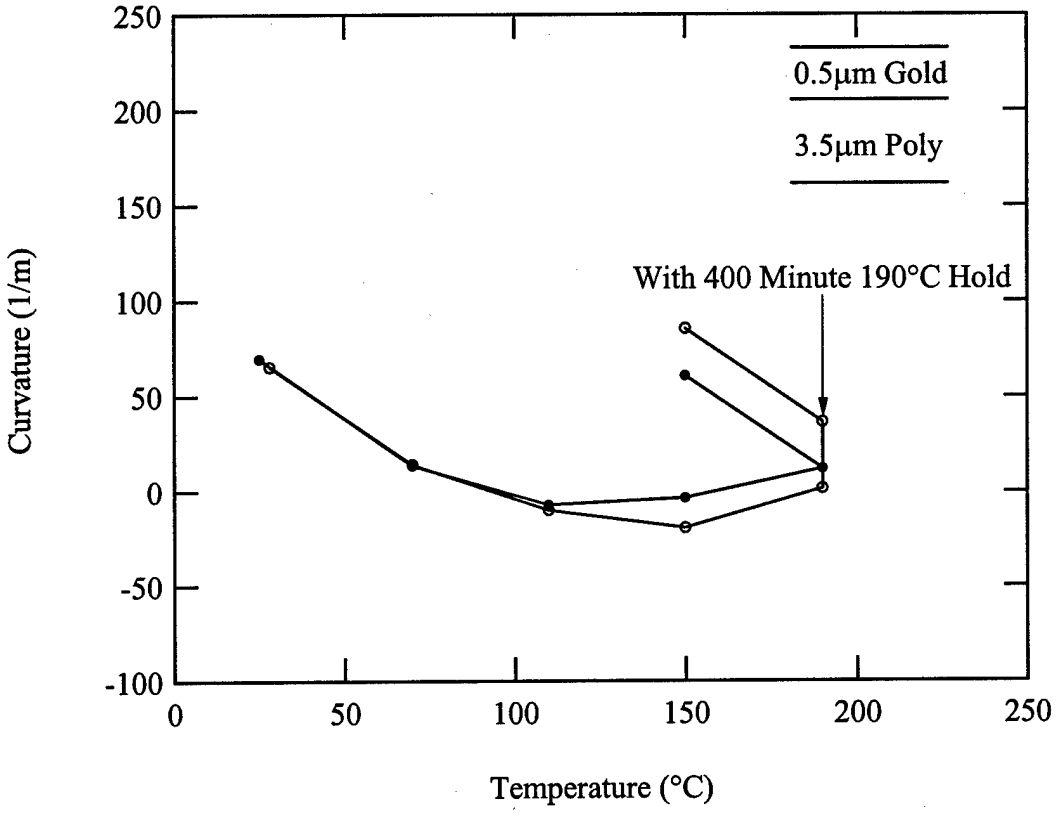

Figure 14. Initial Curvature for 190°C Max, 150°C Hold with and without 400 Minute 190°C Hold

follow the same linear temperature curvature relationship when being cooled back to 150°C. The curvature is shifted up due to the recovery during the 400 minute hold,

but the slope of the linear relationship is the same. The results of the isothermal hold are much different between the two sets of beams. The beams that were not held at 190°C during the initial thermal cycling creep only slightly during the first few hours, then show no creep during the bulk of the hold then recover slightly near the end of the hold period. The beams that were held at 190°C for 400 minutes start at a higher curvature due to the recovery process. They immediately start to creep, this initial stage in which the beams experience a rapid loss of curvature lasts for a shorter time than the other experiments. After the initial rapid loss of curvature the beams creep at a steady rate for the remainder of the experiment.

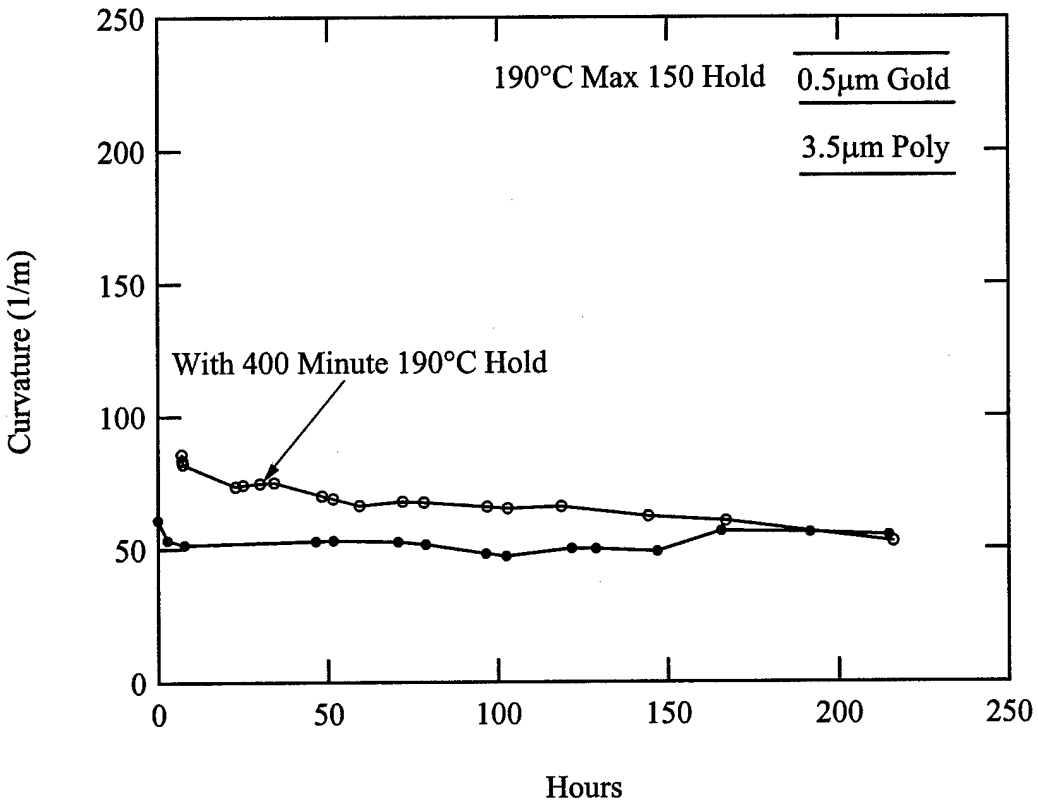

Figure 15. 190°C Max, 150°C Hold Results With and Without 400 Minute 190°C Hold.

3.6 Change in Curvature

The results of three independent sets of data from 190°C maximum, 120°C hold experiments on are shown in Figure 16. This plot was constructed by subtracting each curvature reading from the initial curvature. This represents an easy way to see the change in curvature in both the 3.5μm polysilicon beams and the 1.5μm polysilicon beams. This plot shows that the thinner beams experience a greater change in curvature than the thicker beams. It also makes it very clear that three independent data sets follow the same trends.

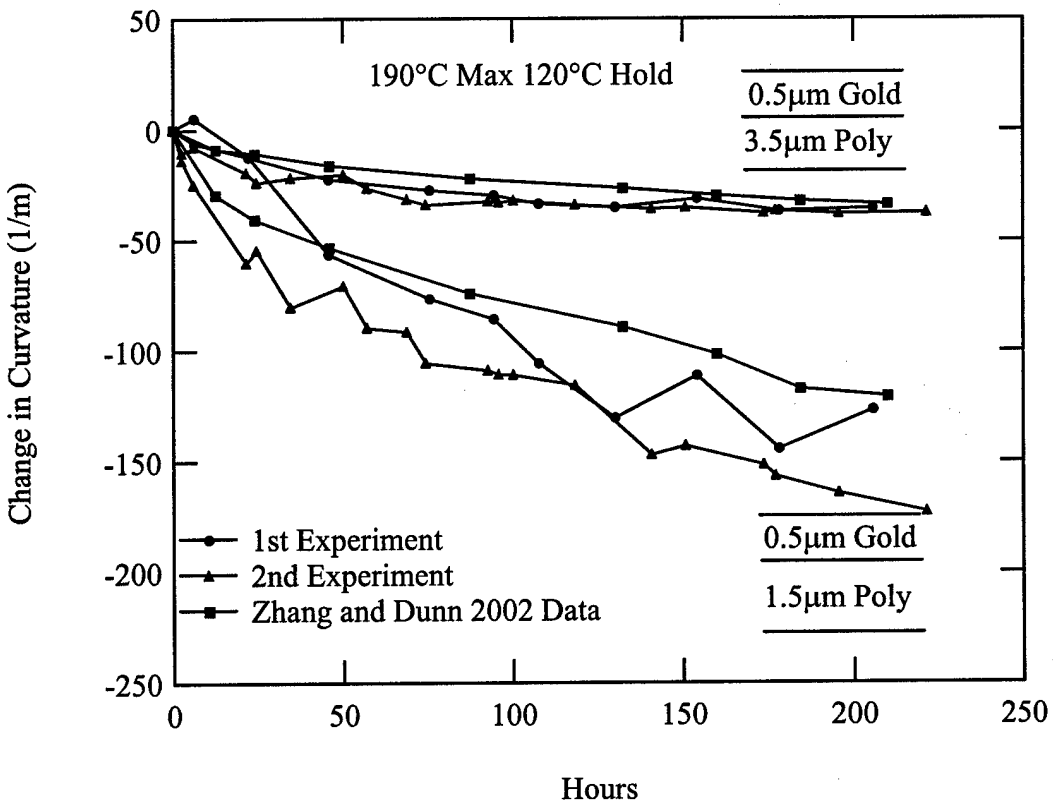

Figure 16. Change in Curvature of 190°C Max and 120°C Hold Experiments.

3.7 Mismatch Strain

Utilizing the equation from Dunn and Cunningham 2003, the mismatch strain from the experiments discussed in section 3.5 is plotted. Figure 17 shows mismatch strain as a function of time for the 190°C maximum, 120°C hold experiments. All of the beams, both the 3.5μm poly silicon beams and the 1.5μm poly silicon beams experience equivelant mismatch strain and change in mismatch strain through the course of the experiment.

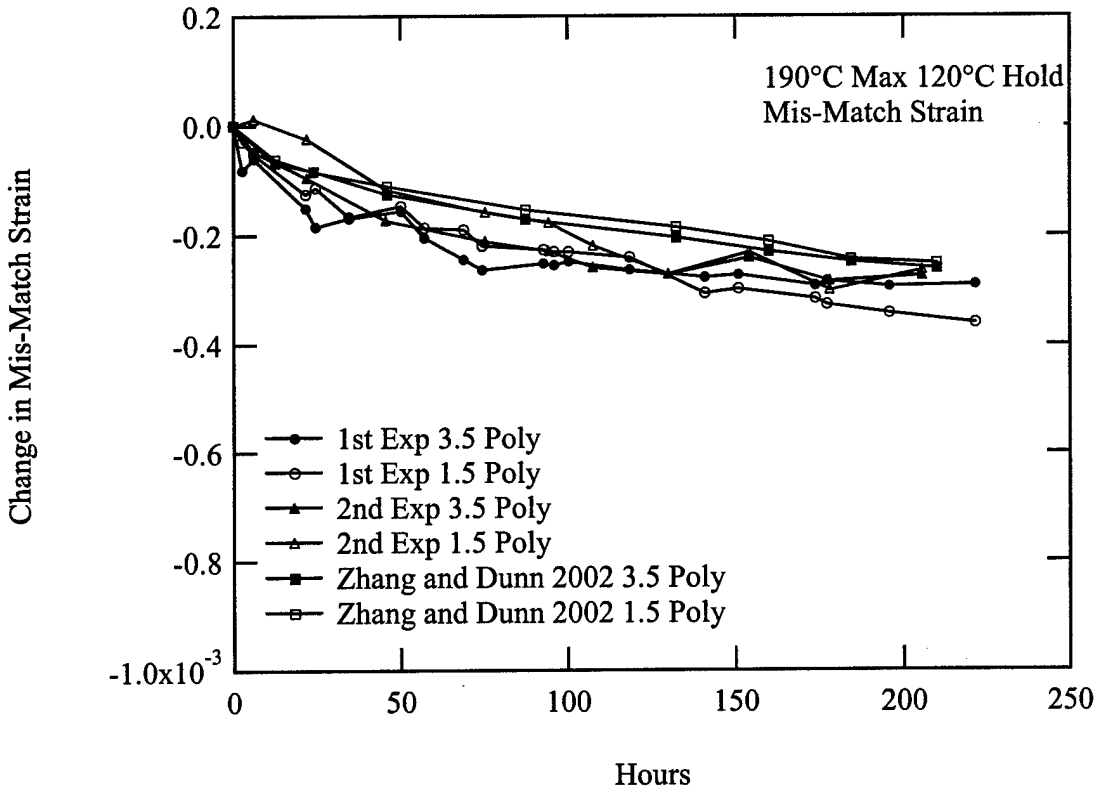

Figure 17. Mismatch Strain for all 190°C Max and 120°C Hold experiments.

4. Microscopy

Beams used in this research were observed using four different microscopy techniques. Interferometry was used to determine beam curvature and surface profile information. This technique was discussed in section 2.2. Scanning electron microscopy (SEM), atomic force microscopy (AFM), and focused ion beam (FIB) microscopy techniques were used to produce images of the beam structures. All three of these techniques allow resolution down to the grain structure of the gold. In an attempt to detect microstructural differences caused by the various isothermal holds. Images were taken of representative as-released beams for comparative purposes. Images were also taken after 200 hour holds at 60, 90, 120, and 150°C. These images could then be compared to detect any differences.

4.1 SEM Images.

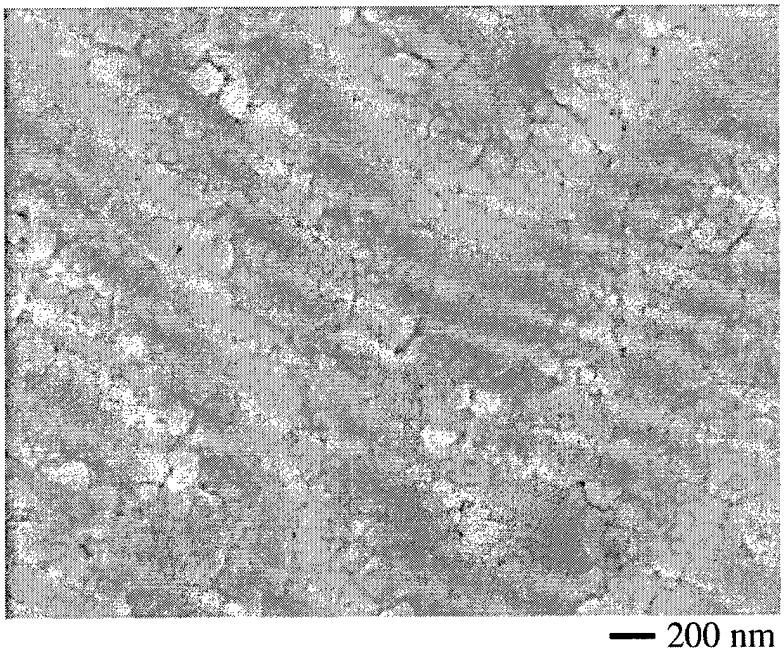

Figure 18. Surface of As-Released Beam

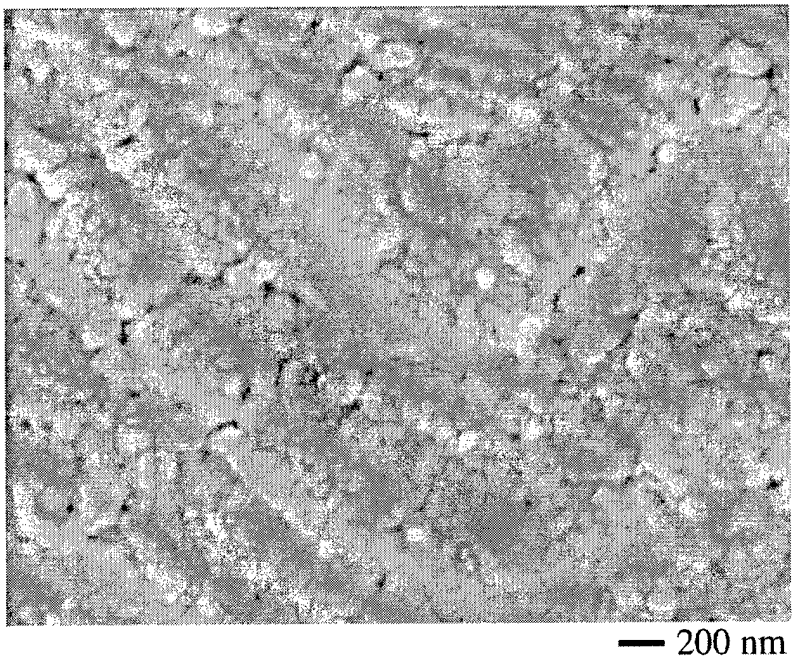

Figure 19. Surface of Beam After 200 Hour 90°C Hold

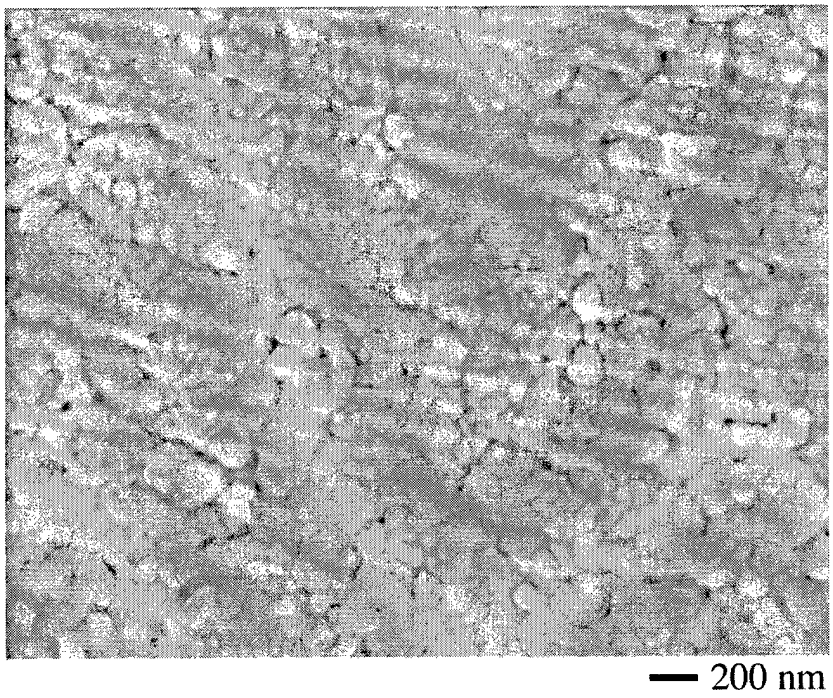

Figure 20. Surface of Beam After 200 Hour 120°C Hold

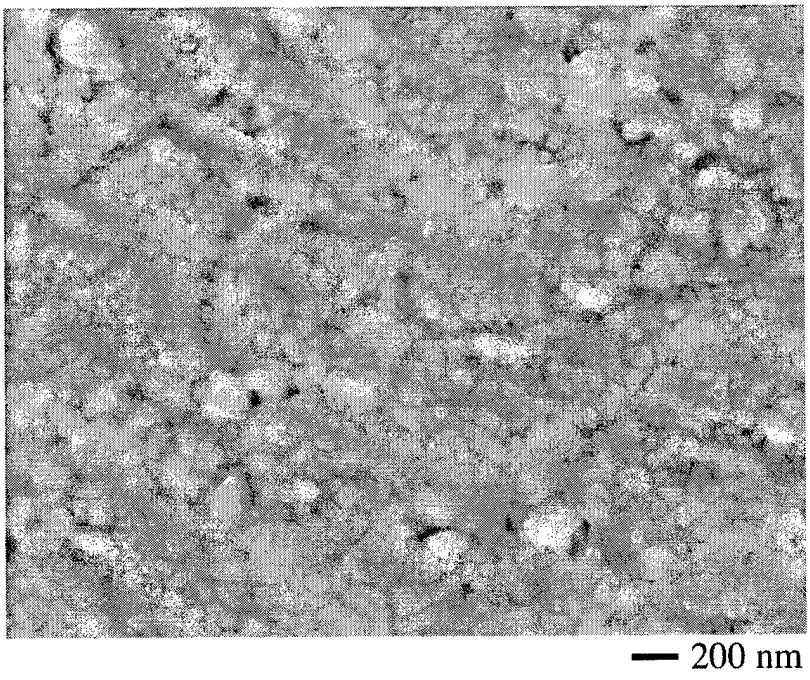

Figure 21. Surface of Beam After 200 Hour 150°C Hold

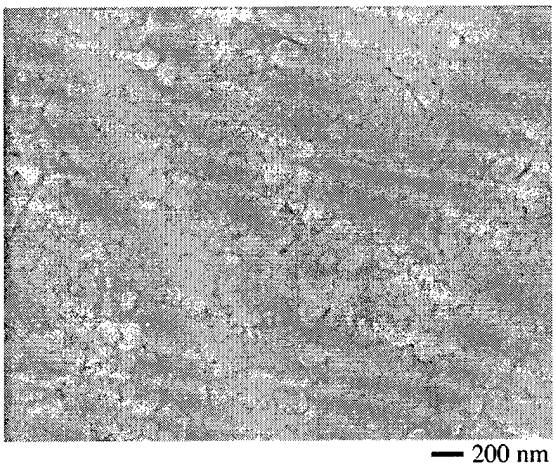

— 200 nm

As released

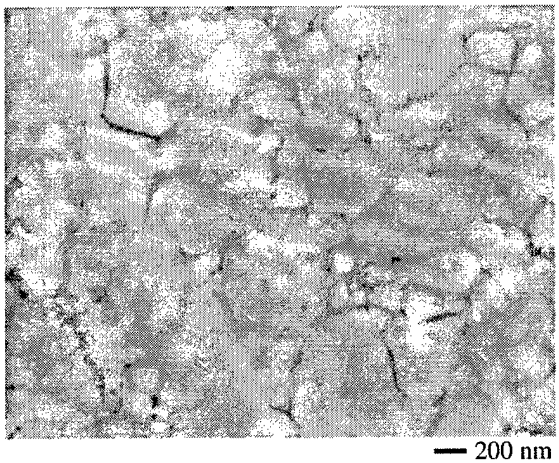

— 200 nm

After 100 hour 180°C Hold

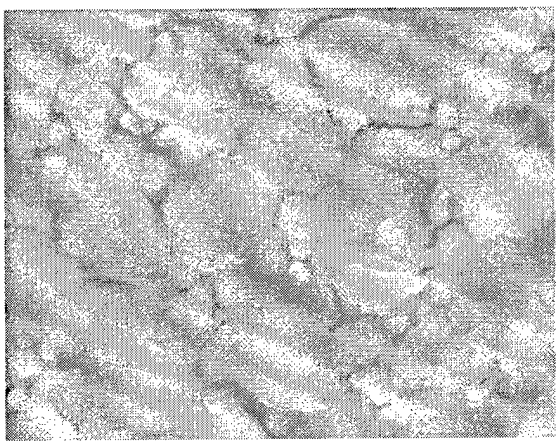

After 6 Hour 225°C Hold

Figure 22. Images of Surface Morphology

4.2 AFM Images

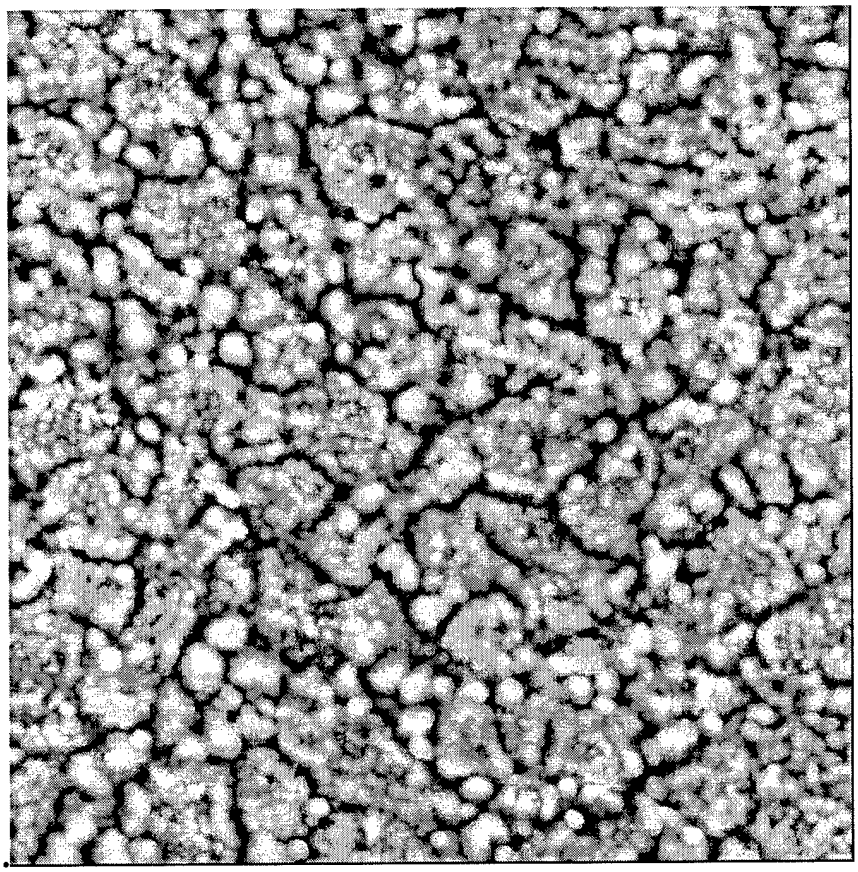

Figure 23. 5μm x 5μm Surface of As-Released Beam

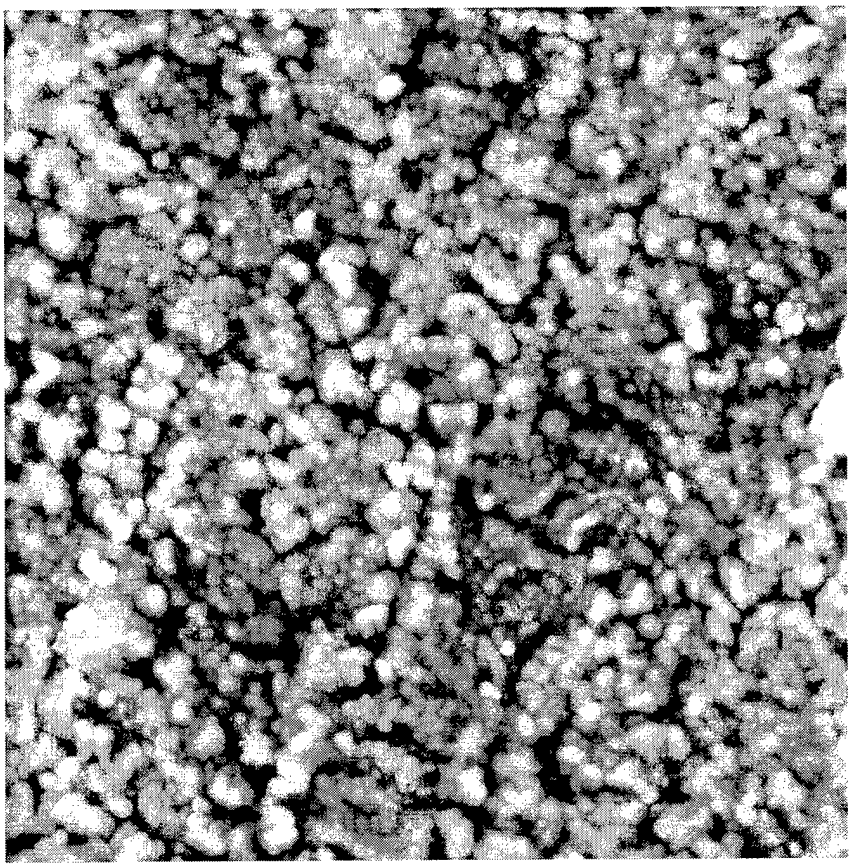

Figure 24. 5μm x 5μm Beam Surface After 200 Hour 90°C Hold

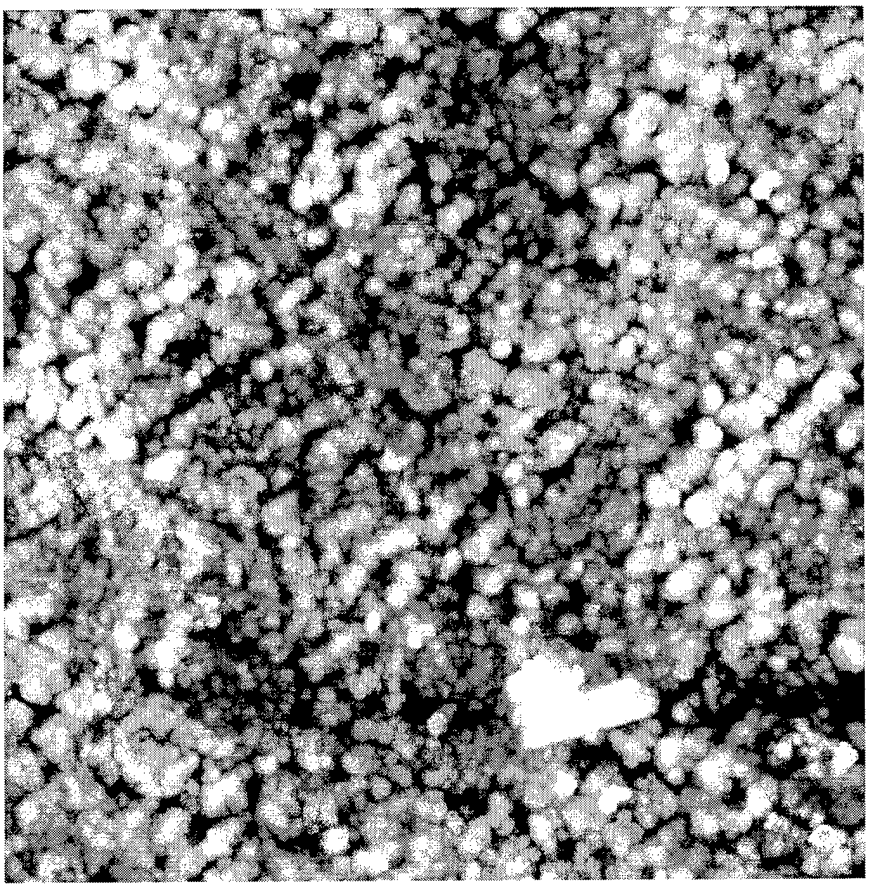

Figure 25. 5μm x 5μm Beam Surface After 200 Hour 120°C Hold

4.3 FIB Images.

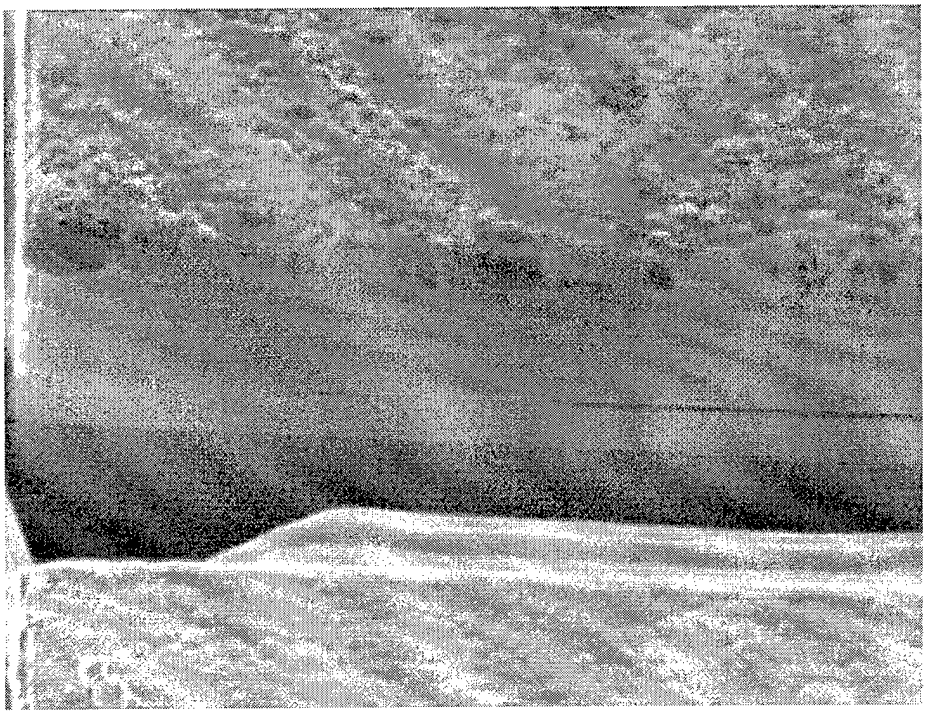

Figure 26. Cross Section Image of As-Released Beam

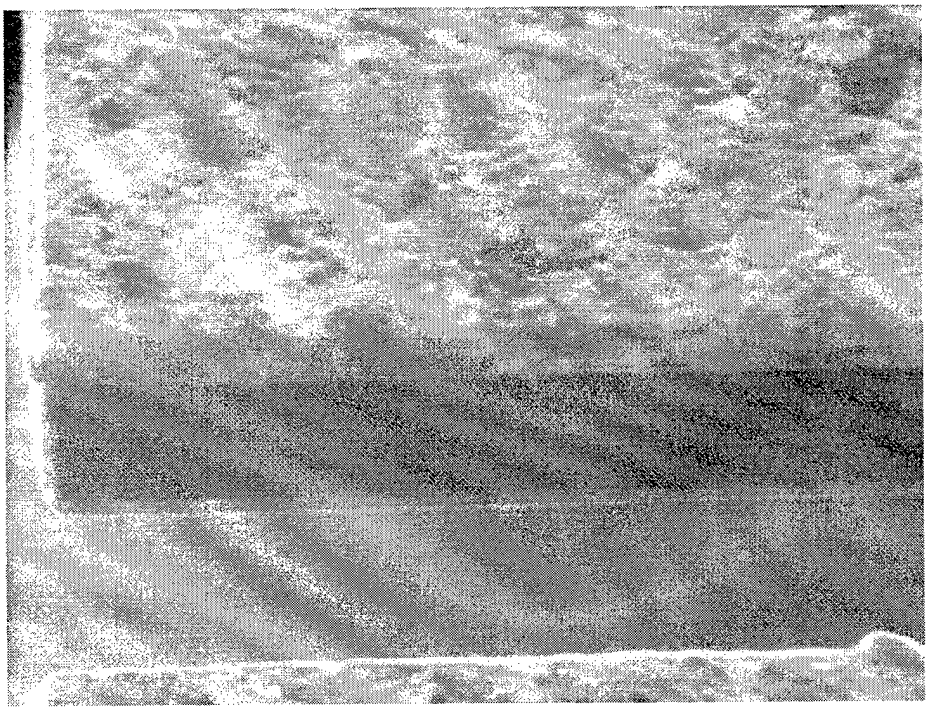

Figure 27. Cross Section Image of Beam Held at 120°C for 2000 Hours

5. Discussion

5.1 Classical Creep

Creep is traditionally defined as time dependent inelastic deformation caused by stress and elevated temperature. In bulk materials, creep is usually not a problem unless the material is held at an elevated temperature, approximately 30% of its melting temp.(Callister 1997) In typical creep experiments, macro scale specimens are held at an elevated temperature and are subjected to a constant stress or strain and the evolution of the other variable is measured. Materials display three stages of creep; primary, secondary or steady state, and tertiary.

Many different deformation mechanisms occur simultaneously during the creep process. Most of these mechanisms have been identified for macro scale material samples (Frost and Ashby 1982), but the mechanisms responsible for creep and their activation parameters in thin films have not been fully identified.

5.2 Creep in Bi-Layer MEMS Beams.

From the research conducted for this thesis we have found convincing evidence to classify creep in gold on polysilicon MEMS beams into two regimes, each having various mechanisms responsible for the beam curvature evolution. Figure 28 summarizes the findings of this research in a flow chart. The two regimes are divided

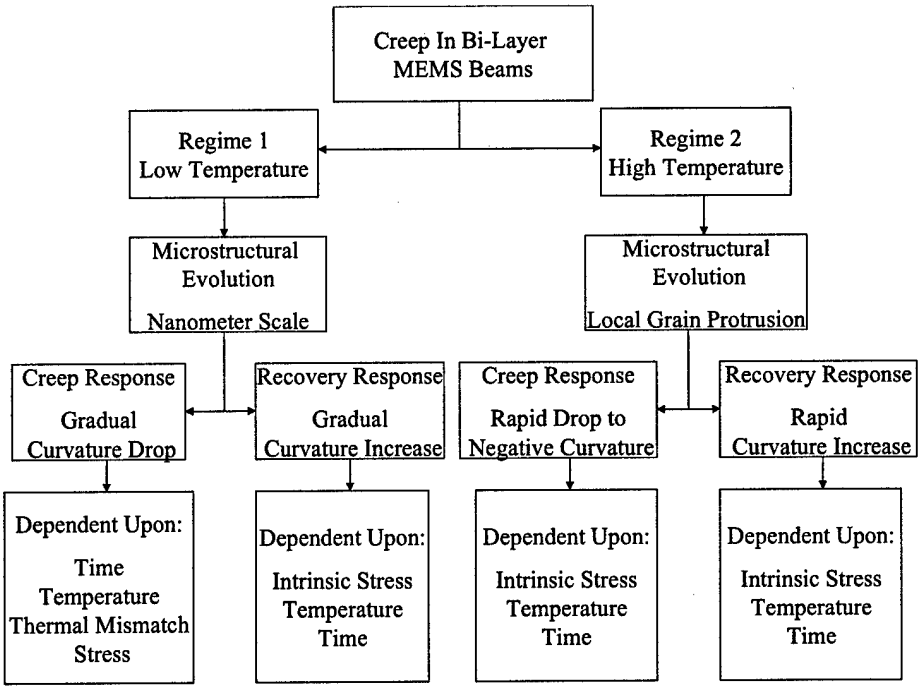

Figure 28. Discussion Summary Flowchart.

into a low temperature regime (regime one) and a high temperature regime (regime two). The main difference between the two regimes is the driving mechanism for creep. It was found that regime two displayed a much higher creep rate than regime one. Through microscopy it was determined that the surface of samples in regime had significant surface smoothing and grain boundaries became more defined. Regime one showed no such microstructural changes. These different driving mechanisms will be discussed further in their respective sections.

5.2.1 Regime One

The first creep regime is the lower temperature regime which spans from approximately room temperature to 190°C. The division between regime one and

two is not an exact point. This division also has a time dependence. It is more convenient to discuss this division further during the regime two section.

There are two mechanisms responsible for beam curvature evolution during the first regime. A creep mechanism, which is responsible for the loss of curvature, and a recovery mechanism, which is responsible for the beam attempting to increase its curvature. It is thought the creep mechanism is either dislocation activity or short range atomic migration based, or a combination of the two. Microscopy imaging to grain structure resolution reveals no significant differences between the grain structure of as-released beams and beams held at various temperatures for 200 hours. (See Figures18-21 and 23-27).

SEM and AFM surface images show no structural differences at the surface of the beams, and FIB imaging shows no change through the cross-section of the beam. Is evident that some mechanism is driving or allowing the creep to take place in the beams. Because microscopy thus far has revealed no conclusive evidence at the scale of observation, smaller scale phenomena must be occurring. Imaging from the next higher level of microscopy, transmission electron microscopy (TEM), will be necessary to confirm dislocation motion or atomic scale diffusion.

Creep in the beams is driven by temperature and stress. High temperature and high stress result in high creep rates. In the bi-layer beams these two factors are inversely proportional. Higher temperature, which would help drive creep, results in a lower stress and lower curvature. Conversely, higher stress, and higher curvature, is driven by lower temperatures, which impedes the creep processes. It is unclear at

this time which of these two factors play a bigger role in the bi-layer creep process, as these variables were not separated in this study.

The second mechanism present in regime one is a recovery mechanism. While creep mechanisms allow a reduction of tensile stress in the gold, recovery mechanisms cause an increase in the stress. Recovery will cause the beam to curve upward to a higher stress state. This recovery mechanism is driven by the microstructure of the gold trying to achieve a lower energy state, this is an intrinsic stress evolution. This recovery is most evident in figure 29. These beams are heated directly to their hold temperatures of 90°C and 190°C. If you

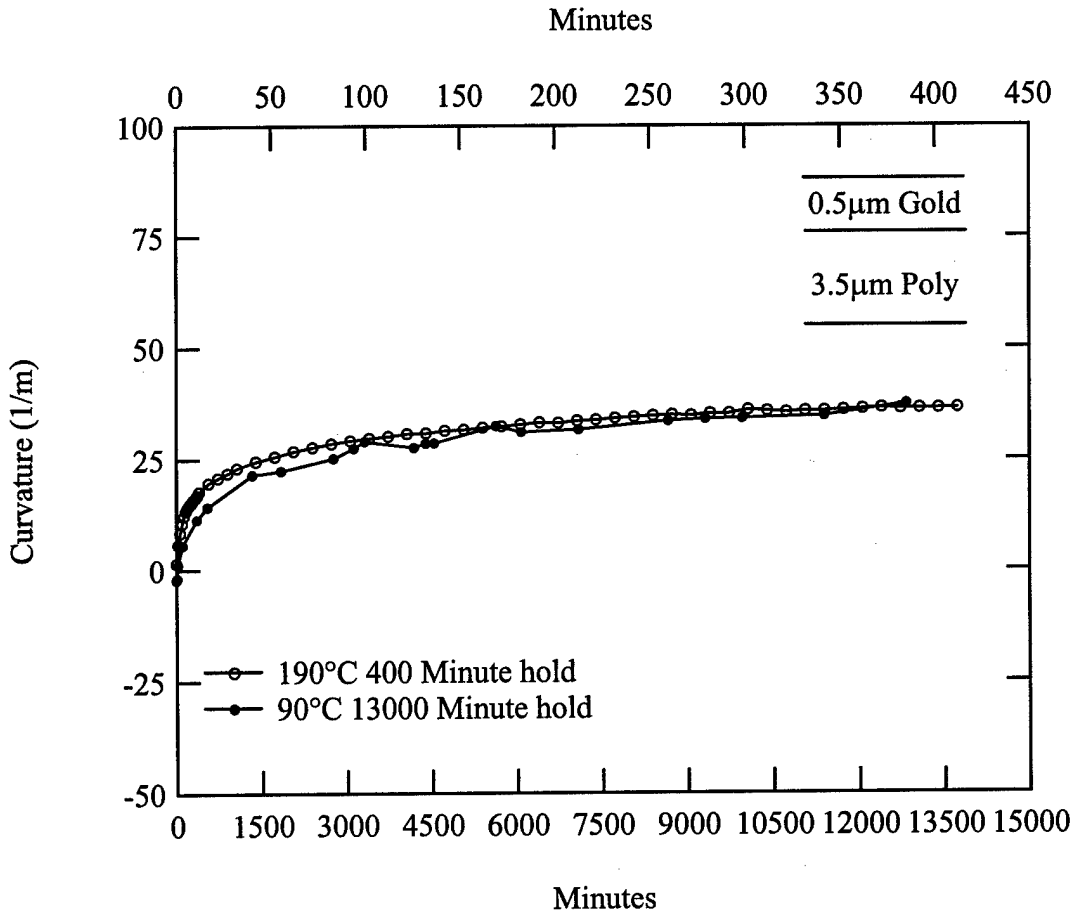

Figure 29. Curvature Recovery at 90°C and 190°C

follow the heating path along the initial thermal cycling plot in figure 7, the curvature of the beams are near zero when they are heated directly to their hold temperature. They remain at a near zero curvature because they are not cooled from their high temperature. Because the beams are very near zero curvature, no extrinsic stress is available to induce creep. The recovery mechanism is the primary driving force present. As evident from figure 29 both beams recover the same amount of curvature but the beam held at the higher temperature achieves this recovery much faster.

It is evident in several creep experiments that both the recovery and creep mechanisms are active at the same time and compete with each other. Figure 11 shows the results of the 190°C max and various hold temperatures experiment set. In the first four hold experiments, the creep mechanisms are dominating the curvature behavior of the beams. This is evident because in the first four experiments the beams were observed to lose curvature throughout the hold time even though the recovery mechanisms are still occurring. In the fifth experiment, the 150°C hold, the beams were observed to lose curvature for approximately four hours and afterwards did not lose curvature for the remainder of the experiment. Furthermore, at approximately 150 hours the beams experienced a slight recovery in curvature. It should also be noted that from approximately 75 hours to 150 hours, the 120°C hold and the 150°C hold had approximately the same curvature. Because the beams had the same curvature they also will have similar stress. However, because the 150°C beams are being held at a higher temperature, the recovery energy in these beams is

being released at a higher rate than the 120°C beams, and this is evident in the 150°C beams' failure to demonstrate creep.

To further illustrate the interaction between the recovery mechanism and the creep mechanism figure 13 shows the results of the 90°C hold experiment. A very similar behavior is noted between this experiment and the previously discussed 190°C max experiment. In both experiments it was observed that a beam that started with a higher curvature displayed creep throughout the hold period while a beam that started with a lower curvature stopped displaying creep at a very early point in the experiment. In the 90°C hold experiment the beams are heated to different maximum temperatures before they are cooled to 90°C. Beams that are heated to a higher maximum temperature will have more curvature when they are cooled back to the same hold temperature. The beam that was heated to 190°C initially has a higher curvature than the beam that was heated to 160°C. Because the 160°C beam was not allowed to dissipate its recovery energy, it stops creeping at approximately 7 hours into the hold and is then observed to recover slightly throughout the remainder of the hold. It is also observed that from approximately 50 hours to 125 hours the 190°C beams and the 160°C beams have a similar curvature and therefore have similar stress state. The driving factors for the creep mechanism, extrinsic stress and temperature, are roughly the same in this time period. It is thought that because the 160°C beams did not dissipate as much recovery energy as the 190°C beams during the initial thermal cycle, the recovery mechanisms in the 160°C beams eventually overcomes the creep mechanism. The 90°C max beams were discussed earlier in this section. Because the beam was not allowed to dissipate any recovery energy and

starts out at zero curvature and stress, the recovery mechanism dominates the entire hold.

Figure 12 shows the results of the 120°C degree hold experiments. The same observations are noted in this experiment as the previous two experiments. Again the recovery energy in the beam that was heated to a lower maximum temperature is able to override the creep mechanisms. The beams that were heated to a higher maximum temperature and thus having expelled their recovery energy continue to creep throughout the entire hold. It is important to note in these last two experiments the beams are held at the same temperature and therefore the remaining recovery energy is being dissipated at the same rate from all beams. Lower temperature beams have expelled less recovery energy during the initial thermal cycle so the recovery mechanism is able to dominate during the hold.

The beams that were held for 400 minutes at 190°C were then cooled to 150°C and held for 200 hours. Figure 15 shows the results of this experiment plotted on the same graph as beams that were heated to 190°C max then immediately cooled to 150°C. This experiment set shares the same max temperature and hold temperature. Due to the recovery experienced during the hold the beams start at different curvatures. More importantly the beams that experienced the 400 minute hold expended more of their recovery energy than the beams that were cooled immediately. This is evident in figure 15 as the beams that were held, creep through out the hold period. Because these beams expended their recovery energy, creep mechanisms can dominate the behavior of the beam curvature.

5.2.2 Regime Two

The most definitive differences between regimes one and two are the surface microstructure evolution and the curvature response. More defined grain boundaries and a smoothing of surface texture on the surface of the beams characterize this microstructural evolution. This evolution is observed in the SEM microscopy images. Figure 22. It is unclear what mechanism causes this smoothing and grain boundary definition, but both are present in beams that are heated above approximately 190°C. There is not a precise dividing line between regime one and two. When beams are heated above approximately 190°C or if they are held in this temperature range the mechanism that responsible for the surface evolution is activated. The curvature response of the beams that enter regime two is very pronounced and is controlled by a new mechanism. Figure 30 shows the initial response of beams that were

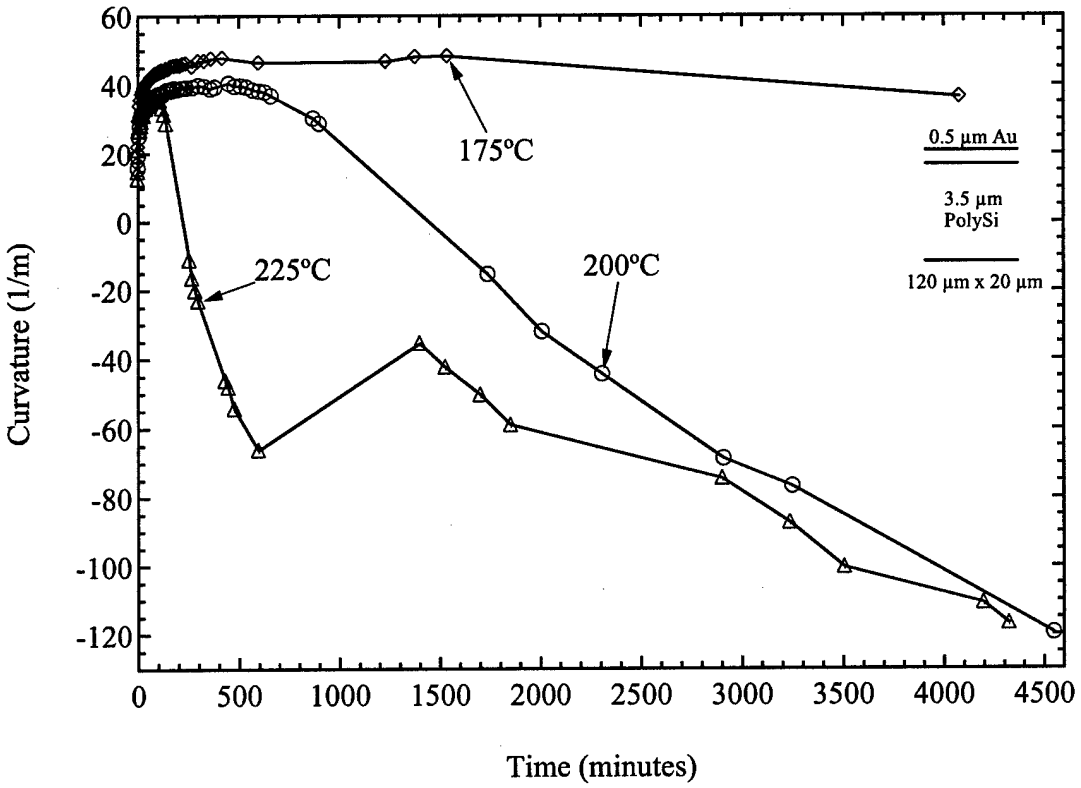

Figure 30. Recovery Behavior at High Temperature (Gall 2003)

held at relatively high temperatures. The beams that were held at 175°C show a recovery and very little creep, these beams remained in regime one. The beams that were held 200°C and 225°C show the initial recovery. This is driven by the same recovery mechanism present in regime one. However, these higher temperature beams enter regime two and the same mechanism that is responsible surface microstructural evolution dominates all other factors in the beam's curvature response. The beams creep at a very fast rate and creep past the zero curvature point. This mechanism is not just allowing the beams to relax to a lower stress state, it is inducing a compressive stress in the gold and forcing the beams to a negative curvature. After the mechanism responsible for the surface evolution has been activated, this creep mechanism dominates over all other factors in the beams

including mismatch strain, resistance from the polysilicon, and recovery mechanisms. The increase in curvature at the beginning of a higher temperature hold is evidence that the recovery mechanism is still active in regime two: however, the energy is dissipated very fast due to the high temperature.

6. Conclusions

Several different stresses act on the beams during thermal cycling and isothermal holds. These stresses can be considered either extrinsic, caused by thermal mismatch, or intrinsic, caused by microstructural changes from within the material. Extrinsic stress, which is due to thermal mismatch and manifested in the beam curvature, is most apparent when changing temperatures cause change in beam curvature. Three different intrinsic stresses can act on the bi-layer beams during the hold experiments. In regime one sub micron scale changes drive a creep mechanism, and in regime two a mechanism that results in the formation of mounds drives the creep. Both regimes experience the effects of an energy driven recovery mechanism. These forces are acting upon the beams at all times. Initial thermal cycling and parameters such as hold temperature and hold time determine which of these forces are dominant.

It is extremely difficult to separate temperature and stress in the bi-layer beams. If an attempt is made to model the curvature behavior in regime one the intrinsic stress must be accounted for. This intrinsic stress caused by the recovery mechanism must be completely dissipated before the beam behavior can be modeled considering only extrinsic stress.

We can conclude from the behavior in regime two that it is very ill-advised operate bi-layer beams in temperature ranges above approximately 190°C. Bi-layer MEMS structures should only be allowed to enter this higher temperature range for very short periods of time. It is critical that the mechanism that causes mounds to form is not activated. Also, due to this mound formation mechanism, accelerated creep tests cannot be conducted in these higher temperature ranges.

7. References

Callister, W.D.,"Materials Science and Engineering an Introduction",4th Ed.,John Wiley and SonsNew York, NY, 1997

Cho, H.S., Hemeker, K.J., Lian, K., Goettert, J., and Dirras, G., "Measured Mechanical Properties of LIGA Ni Structures" Sensors and Actuators, A phys, Vol 103, pp 59-63, 2003.

Dunn, M.L. and Cunningham S.J., "Thermoand Mechanical Behavior of Thin-Film Microstructures", Chapter of "Handbook of Nanotechnology", B. Bhushan, ed., Springer-Verlag, 2003.

Espinosa, H.D., Prork, B.C., and Fischer, M., "A methodology for Determining Mechanical Properties of Freestanding thin Films and MEMS Materials", Journal of the Mechanics and Physics of Solids, vol 51, pp. 47-67, 2003.

Frost, H.J., Ashby, M.F., "Deformation-Mechanisms Maps, The Plasticity and Creep of Metals and Ceramics", Pergamon Press, Elmsford, NY., 1982

Gall, K., Dunn, M.L., Hulse, M., Finch, D. and George, S.M., "Effect of Al_2O_3 ALD Nanocoatings on the Thermo-Mechanical Behavior of Au/Si MEMS Structures," Materials Research, Vol 18, pp. 1575-1587, 2003.

Haque, M.A., Saif, and M.T.A., "Application of MEMS force Sensors for in Situ Mechanical Characterization of Nano-Scale Thin Films in SEM and TEM", Sensors and Actuators, A 97-98, pp. 239-245, 2002.

Haque, M.A., Saif, and M.T.A., "Mechanical Behavior of 30-50 nm Thick Aluminum Films Under Uniaxial Tension", Scripta Materialia 47 pp. 863-867, 2002.

Koester, D.A., Mahadevan, R., Hardy, B., and Markus, K.W., 2001, *MUMPs*™ *Design Rules,* Cronos Integrated Microsystems, A JDS Uniphase Company, *http://www.memsrus.com/cronos/svcsrules.html*

Larsen, K.P., Rasmussen, A.A., and Ravnkilde, J.T., "MEMS Device for Bending Test: Measurements of Fatigue and Creep of Electroplated Nickel", Sensors and Actuaors A, 103, pp. 156-164, 2003.

Nix, W.D., "Mechanical Properties of Thin Films," Institute of Metals Lecture, the Minerals, Metals, & Materials Society, Vol. 20A, 1989, pp. 2217-2245, 1988.

Pamula, V.K., Jog, A., and Fair, R.B., "Mechanical Property Measurment of Thin-Film Gold Using Thermally Actuated Bimetallic Cantilevered Beams" , Modeling and Simulation of Microsystems, (ISBN 0-9708275-0-4), 2001.

Shen, Y.L. and Suresh, S., "Steady-State Creep of Metal-Ceramic Multilayered Materials," Acta matter, Vol. 44. No. 4 pp., 1337-1348. 1996.

Stoney, G.G., "The Tension of Metallic Films Deposited by Electrolysis," Proc. Roy. Soc. London, Vol. A82, pp., 172-175, 1909.

Timoshenko, S., "Analysis of Bi-Metal Thermostats", Journal of the Optical Society of America and Review of Scientific Instruments, Vol. 11, pp., 233-256, 1925.

Zhang, Y. and Dunn, M.L., "Stress Relaxation and Creep of Gold/Polysilicon Layered MEMS Microstructures Subjected to Thermal Loading," in Proceedings of the MEMS Symposium, ASME International Mechanical Engineering Congress and Exposition, Vol. 3, pp. 149-156, 2001.

8. Appendix

Au/Cu Comparison

There are no existing studies on creep of micro scale gold. In order to compare results from the creep experiments performed in this research to existing creep data, we must find data on a similar material. Even though there is no map developed for gold, the mechanical properties of copper are similar enough to gold that comparing our Au/Si creep experiment results to the results of freestanding copper can still be meaningful. Furthermore the results obtained from our gold on silicon creep experiments can be compared to the properties of freestanding copper film as presented by Haibo Huang doctoral thesis 1998.

Justification for comparing gold to copper is due to the similar mechanical properties. The most important of which is the stacking fault energy.

	Cu	Au	
Stacking fault energy	78	33	mJ/m^2
Melting temperature	1356	1337	K
Crystal structure		FCC	FCC
Modulus of elasticity	102	79	GPa
Poission's ratio		.33	.42

Thermal mismatch stress is determined from work done by Zhang and Dunn (year). Their work shows a stress gradient exists in the gold film. Using stress data from the elastic region, an average stress in the film due to a 100°C temperature change is used as a ratio to calculate stress in the beams at each different experimental temperature. The ratio used to calculate the stresses is as follows:

$$\frac{112.5\,MPa\,(\sigma)}{100\,°C\,\Delta T} = \frac{X\,MPa\,(\sigma)}{Y\,°C\,\Delta T}$$

Which yields the results:

Hold temperature	60 °C	90 °C	120 °C	150 °C	180 °C
Change in temperature	130°	100°	70°	40°	10°
Stress (Mpa)	143.25	112.5	78.75	45	11.25

Stress due to simple tension must be converted to normalized Shear Stress to plot it on the creep deformation map. In order calculate shear stress we use an equation given by Frost and Ashby. For simple tension, shear stress is related to tensile stress by:

$$\frac{\sigma}{\sqrt{3}} = \sigma_s$$

Which yields the results:

Hold temperature	60 °C	90 °C	120 °C	150 °C	180 °C
Shear stress (Mpa)	84.43	64.95	45.46	25.98	6.495

To normalize the shear stress it must be divided by the shear modulus. Shear modulus is related to modulus of elasticity and Poision's ratio by:

$$\mu = \frac{E}{2(1+\nu)}$$

Where modulus of elasticity and Poision's ratio equal:

E_{Au}=79GPa =79,000 MPa □$_{Au}$=.42

Shear Modulus equals:

G or μ ≈27,816 MPa

Normalized Shear stress:

Hold temperature	60 °C	90 °C	120 °C	150 °C	180 °C
Normalized Shear stress (MPa)	3.035E-3	2.335E-3	1.634E-3	9.34E-4	4.044E-4

The creep mechanisms maps plot the normalized shear stress verses the homologous temperature. The homologous temperature is temperature divided by the melting temperature of the material. (Absolute temperature units). Converting all the hold temperatures to Kelvin and dividing by the melting temperature in Kelvin:

Hold temp °C	60	90	120	150	180
Hold temp K	333	363	393	423	453
T_{melt} K	1337	1337	1337	1337	1337
T/T_{melt}	.25	.27	.29	.32	.34

With shear stress and homologous temperature it is possible to plot gold on silicon creep experimental results on a creep deformation map. In order to further understand the mechanisms occurring in the gold on silicon creep experiments we can also look at the strain rate. Strain rates cannot be measured directly on the gold on silicon beams. We must utilize the curvature and change in curvature to determine the mismatch strain. It is important note that there are distinctly different creep stages in the collected data. The first stage is primary creep which has a much faster creep rate. In the second stage the plotted results become nearly linear and creep rate slows down considerably.

Using data from the 190 degree maximum temperature and various hold temperature experiments, the average strain rate for the entire hold and the strain rate for the steady state creep are calculated.

Average strain 190 Max 3.5 silicon (Entire hold)

60 hold	90 hold	120 hold	150 hold	180 hold
□□	□□	□□	□□	□□
0.0003577	0.000144704	0.0002239	0.00032955	0.000236604
0.0358%	0.0145%	0.0224%	0.0330%	0.0237%

Average strain rate 1/s 190 Max 3.5 silicon (□□ / Entire Hold Time)

60 hold	90 hold	120 hold	150 hold	180 hold
ε	ε	ε	ε	ε
4.968E-10	2.00978E-10	3.109E-10	4.5771E-10	3.28617E-10

Average strain 190 Max 3.5 silicon (Steady State)

60 hold	90 hold	120 hold	150 hold	180 hold
□□	□□	□□	□□	□□
2.99E-05	3.77899E-05	2.526E-05	0.0001871	0.000361351
2.99E-05	3.77899E-05	2.526E-05	0.0001871	0.000361351

Average strain rate 1/s 190 Max 3.5 silicon (□□ / Steady State Hold Time)

60 hold	90 hold	120 hold	150 hold	180 hold
ε	ε	ε	ε	ε
4.746E-11	5.9984E-11	4.009E-11	2.9699E-10	5.73574E-10

The primary stage lasts from the beginning of the experiment to approximately 25 hours. The secondary or steady state creep stage lasts from 25 to 200 hours.